General Disclaimer

One or more of the Following Statements may affect this Document

- This document has been reproduced from the best copy furnished by the organizational source. It is being released in the interest of making available as much information as possible.

- This document may contain data, which exceeds the sheet parameters. It was furnished in this condition by the organizational source and is the best copy available.

- This document may contain tone-on-tone or color graphs, charts and/or pictures, which have been reproduced in black and white.

- This document is paginated as submitted by the original source.

- Portions of this document are not fully legible due to the historical nature of some of the material. However, it is the best reproduction available from the original submission.

Produced by the NASA Center for Aerospace Information (CASI)

DOE/NASA CONTRACTOR REPORT

DOE/NASA CR-150604

PUMP/CONTROL SYSTEM MINIMUM OPERATING COST TESTING

Prepared by

Department of Mechanical Engineering
Tennessee Technological University
Cookeville, Tennessee

Under Contract NAS8-31564 with

National Aeronautics and Space Administration
George C. Marshall Space Flight Center, Alabama 35812

for the U. S. Department of Energy

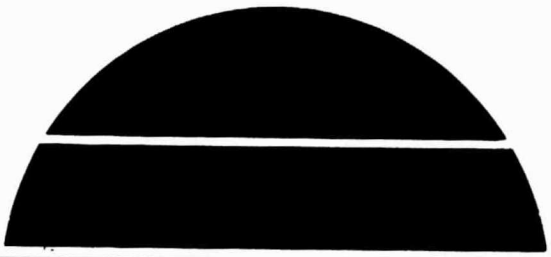

(NASA-CR-150604) PUMP/CONTROL SYSTEM MINIMUM OPERATING COST TESTING (Tennessee Technological Univ.) 72 p HC A04/MF A01 CSCL 10A

N78-20617

Unclas
G3/44 11851

U.S. Department of Energy

Solar Energy

TECHNICAL REPORT STANDARD TITLE PAGE

1. REPORT NO.	2. GOVERNMENT ACCESSION NO.	3. RECIPIENT'S CATALOG NO.
DOE/NASA CR-150604		

4. TITLE AND SUBTITLE	5. REPORT DATE
Pump/Control System Minimum Operating Cost Testing	December 7, 1977
	6. PERFORMING ORGANIZATION CODE
7. AUTHOR(S)	8. PERFORMING ORGANIZATION REPORT #
9. PERFORMING ORGANIZATION NAME AND ADDRESS Department of Mechanical Engineering Tennessee Technological University Cookeville, Tennessee	10. WORK UNIT NO.
	11. CONTRACT OR GRANT NO. NAS8-31564
12. SPONSORING AGENCY NAME AND ADDRESS National Aeronautics and Space Administration Washington, D. C. 20546	13. TYPE OF REPORT & PERIOD COVERED Contractor Report
	14. SPONSORING AGENCY CODE

15. SUPPLEMENTARY NOTES

This work was done under the technical management of Dr. William R. Humphries, George C. Marshall Space Flight Center, Alabama.

16. ABSTRACT

This study was not directed at ranking or recommending specific pumps available for use in solar systems. The primary purpose was to assess the trends in factors affecting energy usage in typical prime movers which might be used in liquid transport solar systems. Since this is not a comprehensive study, using only arbitrarily selected pumps, the reader is cautioned against selecting a pump from this report based purely on the data contained herein. In particular, important aspects of pump selection such as durability, materials compatibility, safety, and other significant features were not addressed in this study. Only a small arbitrary selection of a representative cross section of available pumps was tested; therefore, other pumps may exist which are superior to those discussed.

17. KEY WORDS	18. DISTRIBUTION STATEMENT
	Unclassified-Unlimited William A. Brooksbank WILLIAM A. BROOKSBANK, JR. Manager, Solar Heating and Cooling Proj Ofc

19. SECURITY CLASSIF. (of this report)	20. SECURITY CLASSIF. (of this page)	21. NO. OF PAGES	22. PRICE
Unclassified	Unclassified	71	NTIS

For sale by National Technical Information Service, Springfield, Virginia 22151

TABLE OF CONTENTS

INTRODUCTION

In systems utilizing fluid handling pumps, significant wastes of energy may result from improper pump selection or from inefficiencies in the pump and pump-drive-train combination. The effect of these types of energy losses on an energy conscious nation were addressed in reference [1]* where a range of pump efficiencies of 10 to 90% were identified. While most of the attention in reference [1] was devoted to systems such as domestic water wells and automotive circulation systems, an obvious need to improve electric motor operation also exists. The Fluids Engineering Division of ASME has also identified the problem of energy loss in pumps in reference [2]. It was stated that turbomachinery had replaced positive displacement pumps in many applications and that a high demand existed for improved efficiency.

The study reported herein was initiated to ascertain characteristics of typical "off-the-shelf" pumping systems which might be used in solar systems. All pumps which were examined were of the type and size to meet the range of operating parameters which were anticipated in the solar collector and/or solar load subsystem flow loops of residential-sized solar heating and cooling systems. Establishing variation of pump system overall efficiency with size and type of pump was a primary goal. Overall pumping system efficiency, which includes contributions from the pump, the coupler, and the motor, was also examined. In a number of cases each of these contributions were determined.

Some of the factors which influence pump selection for solar installations include type of collector, area of collector, type of fluid being circulated through the collector and the temperature rise of the circulating fluid.

*Numbers in brackets designate references listed at the end of the report.

For each particular installation, specific attention must also be given to factors such as the piping configuration, flow obstructions, inlet and exit conditions at the storage tank and the difference in elevation between the storage tank and the top of the collector. The pump sizes normally encountered in residential-sized systems range from one-twentieth horsepower to one horsepower.

Since a solar system may be expected to operate for fifteen to twenty years, a pumping system which is matched to the needs of the solar elements while operating at its peak efficiency can provide a significant savings in terms of operational costs. This savings may be reflected in the economic feasibility of solar energy.

Pump sizes which have been used on liquid transport solar systems vary over a wide range. For small hot-water systems, pumps as small as 1/20 hp have been used with sizes up to 1 hp not uncommon for larger residential heating applications. Since sizes are available only in discrete horsepower increments, it is often times impossible to perfectly match the pump to the flow loop requirements. The designer should, however, make every effort to select a pump properly matched to the system requirements, which operates at or near the pump's peak efficiency. In order to achieve this goal the designer needs reliable efficiency data for the pump. These data must be in the form of overall pump train efficiency (i.e., includes pump, motor and coupler) versus head capacity capability.

Unfortunately, a review of manufacturer literature indicates only limited data are available. Efficiency data seem to be available primarily for larger pumps. Those companies that do supply data for the smaller sizes of interest in this study usually supply only pump efficiency versus head-capacity data, rather than overall efficiency data. Using physical scaling laws to alter the available large pump size data is not an acceptable technique in many cases

because prediction techniques are inexact when scaling from large to very small sizes.

In support of the overall objective of this study, which was to ascertain characteristics of typical off-the-shelf pumping systems, several phases of work were involved and each is reported herein. A review of the theoretical background of pump types and operating characteristics is presented in the appendix along with brief discussions of noise and cavitation considerations. The results of an extensive experimental program on determining the efficiencies of a variety of pumping systems are given. The results of an earlier task have been combined along with those obtained from this study so that all cases are documented herein. Pump noise and its relationship to pump type and size was examined experimentally and the results are presented. Comparison of pump-flow control via throttling and by-passing techniques is also discussed.

BACKGROUND CONSIDERATIONS

Introduction

Efficiency data for pumps smaller than one horsepower are not always provided by manufacturers. A representative of one pump manufacturer stated: "Efficiency data for small pumps were not presented because everyone knew that the efficiencies were low." Although pump operating cost is not a major expense for solar systems, it certainly deserves consideration when a long life (i.e., of the order of fifteen years or more) is expected. One of the first steps of this work, therefore, was a study of the efficiency of small pumping systems from 1/12 hp up to 1 horsepower which are typical of most residential solar system applications. Twenty pump companies were contacted and study goals selected based on the data returned.

One conclusion of the preliminary studies was that a typical solar house would use either the centrifugal pump or the rotary gear pump. The cam and piston, screw, and vane pumps were essentially identical in performance to the gear pump, but they were generally more expensive. The wobble-plate pump offered no advantage over the gear pump for solar applications, and it was much more expensive. Axial flow pumps could not generate the desired head, while mixed flow pumps capable of the desired head performed essentially like centrifugal pumps. General features of the aforementioned types of pumps are outlined in the appendix.

Three items influence the accuracy of determining overall pump performance using analytical techniques and manufacturing data. These items are 1) overall efficiency (with separation of the pump, motor, and coupler efficiencies desirable where possible), 2) scaling of data from available size data to the smaller sizes of interest, and 3) effects of cavitation on head capacity and efficiency.

The efficiency of the electric motor, coupler and pump is often not separable as desired because they are fabricated together. The theoretical scale modeling equations which are outlined in the appendix are typically used to predict pump characteristics. Unfortunately, the use of scaling laws can introduce size effect errors. Typically, no consideration of the effect of cavitation is presented by manufacturers. Complicating this, it is extremely difficult to predict the level of performance degradation resulting from occurence of this phenomenon, even when data are available.

Power Consumption Evaluation

Unfortunately, most pump suppliers who provide efficiency data give only the pump component efficiency data. These have probably been incorrectly used in many instances to estimate pump power consumption by using the expression

$$\text{Power Consumed} = \frac{\text{Fluid Power}}{\eta_p} \tag{3.1}$$

where η_p denotes the pump component efficiency. This is incorrect since the overall pump train efficiency η_o in general is a result of the product of the pump efficiency, the coupling efficiency and the efficiency of the electrical motor. More specifically, the power consumed is given by

$$\text{Power Consumed} = \frac{\text{Fluid Power}}{\eta_p \times \eta_c \times \eta_e} \tag{3.2}$$

or

$$\text{Power Consumed} = \frac{\text{Fluid Power}}{\eta_o}$$

where η_o denotes the overall efficiency determined by the product $\eta_p \times \eta_c \times \eta_e$.

Use of Available Pump Data

Because of some of the aforementioned uncertainties associated with some data obtained from manufacturers, it is difficult to determine the individual

contributions to overall efficiency. Usually, head-capacity data and efficiency data for centrifugal pumps are given in the form shown in Figure A.4. Characteristic pump curves shown in references [3-10] were examined to obtain example values of efficiency and flow rate. In some cases, the curves examined represented correlations of data from a range of pump sizes. Table 3.1 shows the peak efficiency values obtained from selected curves in these references. The data does not necessarily apply to any particular pump size, and they are included here simply to illustrate the range of peak efficiencies which may be reported.

Table 3.1. Example Centrifugal Pump Data

Reference	Q, gpm	η_p, %
[3]	145	58
[4]	500	75
	100	70
[5]	100	68
[6]	100	66
[7]	63	40
	32	30
[8]	1000	82
	500	76
	100	63
[9]	2800	78
[10]	500	75
	100	65

Reference [4] also gave some overall efficiency trends for centrifugal pumps and their associated electrical motors. Table 3.2 shows some of these representative values.

Table 3.2. Example Overall Efficiencies

Motor, HP	η_o, %
5	56
15	61
20	65
40	62

ORIGINAL PAGE IS
OF POOR QUALITY

Some remarks in the literature indicate that axial pumps generally have higher efficiencies than those for centrifugal pumps, specifically in reference [5]. However, there is some disagreement since reference [8] gave a range of efficiencies for axial pumps from 50 to 70%. The efficiency of rotary-gear pumps was given in reference [9] to be constant at most capacities (one particular pump had a value of 72%).

Efficiency Prediction Problems

Based on the ideal scale modeling equation (A.17), it was observed that the efficiencies of centrifugal pumps obviously show a trend toward decreased efficiency with decreasing size. Three major factors influence the efficiency: leakage back through the impeller, mechanical losses, and kinetic losses (see references [7] and [10]). The percent leakage can be made to remain relatively constant for large systems, but the precision of fit between the impeller and housing becomes limited at the smaller sizes by the smoothness of the pump surfaces. These effects contribute to size effects so that the smaller the pump the greater the relative loss associated with leakage. The mechanical friction losses also decrease with size and load. The ratio of these losses to the power required may also increase in small pumps as a function of surface finish.

The kinetic losses (or hycraulic losses) occur on the inlet section, the rotor, the diffuser, and the outlet section [7]. The head loss in pipes at inlet and outlet is related to the relative roughness of the pipes as illustrated on the Moody diagram [6]. Since the roughness of the piping and rotor are relatively constant, the relative roughness increases with smaller pumps. The Moody efficiency factor was developed to predict the reduction in the efficiency due to kinetic losses of a small pump with respect to a large pump [6]. The resulting expression is

$$\eta_m = 1 - (1 - \eta_L)\left(\frac{d_L}{d}\right)^{0.45}\left(\frac{N_L}{N}\right)^{0.2} \qquad (3.3)$$

where the subscript L denotes the larger pump. The efficiency of small pumps, particularly poorly-designed ones, can be much less than that given by equation (3.3). The diffuser section can also be a problem with smaller pumps because there is less time and space available to recover the kinetic energy. The magnitude of these losses is difficult to assess analytically and can be determined only by measuring their net effect on efficiency.

Pump Train Efficiency

Direct coupling of the electric motor to a pump is common in small pumps; therefore, it is not always possible to experimentally evaluate the pump efficiency independent of the motor and coupler. This is particularly true for the magnetically-driven pumps. Consequently, for intimately coupled pumps, electric motor efficiencies must be known before the pump efficiency can be evaluated. Typical values of electric motor efficiencies were given in reference [6] to be between 80 and 95%. However, these efficiencies are appropriate only for large electric motors and are too high for the smaller pumps of interest in this study (i.e., less than 1 hp).

Efficiency Determination from Manufacturer's Data

Before any tests were conducted in this study, a survey was made of data on a variety of pumps. In this section, data from three different pump manufacturers were used. Table 3.7 is for a positive displacement pump while Tables 3.4 to 3.6 are for centrifugal pumps. The methods used in determining tabular data are given when the data was not directly extracted from the manufacturer's data.

Most of the manufacturer's data for small centrifugal pumps do not include the efficiency data, and others present only limited information. The Price Pump Company gave a figure similar to Figure A.4 with the data shown in Table 3.3.

Table 3.3. Representative Centrifugal Pump Data, Price Pumps

$\dot{Q}$, GPM	η_p, %
30	40
20	30
10	20

These values tend to agree with the experimental data collected during this study and presented later in this report.

If the rated value of the electric motor is assumed to be the power consumption, the overall efficiencies can be calculated using performance data from some suppliers. This was done for pump data obtained from Flotec, Inc. Here the overall efficiency was determined by

$$\eta_o = \frac{\dot{Q}(\Delta H)}{HP} \tag{3.4}$$

where the denominator was assumed to be the rated motor power. The results for a variety of sizes of centrifugal pumps are given in Table 3.4. Some data were given for phenolic plastic centrifugal pumps by Flotec where the electric current values were presented. This information is presented in Table 3.5. The overall efficiencies shown in Table 3.5 were determined assuming that the voltage was 120 V and that the power factor was unity.

Overall efficiencies for the Teel ball bearing centrifugal pump was calculated using the method of equation (3.4). The results are given in Table 3.6. Only the maximum efficiency point for each pump was selected for data tabulation. The first pump in Table 3.6 was one of the pumps tested in the experimental phase of this work, and results are given in figure 3.7. Using this same technique, data were also used to calculate efficiencies for Teel gear pumps. Table 3.7 presents these results. Although there are a number of exceptions, it can be seen from these results that the smaller pumps are in general less efficient than larger pumps for similar geometries and operating conditions.

Table 3.4. Overall Pumping, Efficiency Using Flotec, Inc. Data and Assuming a Power Consumption Equal to the Motor Rating

HP	$\dot{Q}$, GPM	ΔH, Ft. Water	η_o
1/12	4.7	20	28.5
1/12	0.7	20	4.2
1/12	1.2	40	14.6
1/8	1.1	20	4.5
1/8	1.8	20	7.3
1/8	2.4	20	9.7
1/8	2.1	40	17.0
1/6	2.6	30	12.7
1/6	3.0	40	18.2
1/6	2.5	50	19.0
1/3	4.8	40	14.6
1/3	8.4	40	25.5
1/3	5.4	50	20.5
1/3	7.1	50	26.9
1/3	3.6	60	16.4
1/4	5.6	20	11.3
1/4	4.8	40	19.4
1/4	2.1	40	8.5
1/4	6.5	40	26.3
1/4	2.8	60	17.0
1/2	7.2	50	18.2
1/2	5.4	60	16.4
1/2	7.6	60	23.1

Table 3.5. Overall Efficiency Estimates for Flotec, Inc. Data on Phenolic Plastic Centrifugal Pumps

$\dot{Q}$, GPM	ΔH, Ft. Water	Current, Amps.	η_o, %
3.7	5	4.6	1.3
3.3	10	4.8	2.2
2.6	20	5.4	3.0
2.1	25	5.6	2.9
1.6	30	5.8	2.6
4.1	5	4.7	1.4
3.8	10	4.9	2.4
2.9	20	5.4	3.4
2.4	25	5.6	3.4
2.0	30	5.8	3.2

ORIGINAL PAGE IS
OF POOR QUALITY

Table 3.6. Teel Centrifugal Pump Data

HP	$\dot{Q}$, GPM	ΔH, Ft. Water	η_o
1/4	6	10	6.1
1/3	17	30	39.4
1/2	20	30	30.3
3/4	47	40	63.4
1	54	40	54.6
1 1/2	66	40	44.5

Table 3.7. Teel Gear Pump Data

Pipe Size	HP	N, RPM	$\dot{Q}$, GPM	ΔP, PSI	η_o
1/8	1/6	1725	1.4	40	19.7
1/8	1/4	1725	1.1	60	15.5
1/4	1/6	1200	2.5	20	17.6
1/4	1/4	1725	3.5	40	32.8
1/4	1/3	1725	3.2	60	33.7
1/4	1/2	1725	2.8	100	32.8
1/2	1/4	900	4.9	20	22.9
1/2	1/3	1200	7.0	20	24.6
1/2	1/2	1200	6.5	40	30.4
1/2	3/4	1725	10.3	40	32.2
1/2	3/4	1200	5.6	80	35.0
1/2	1	1200	5.2	100	30.4
1	1/2	900	12.3	20	28.8
1	3/4	900	12.1	40	38.1
1	1	900	11.5	80	53.8
1	2	1200	15.2	100	44.5
1	3	1725	23.1	100	45.1

Representative Cost Information

The range of prices for centrifugal pumps depends on the material from which the pump is constructed and on whether or not the unit also includes the electric motor. The cost data shown in Table 3.8 were taken from quoted dealer prices and should be representative of the field. Only pumps in the range of 1/3-1/2 hp are covered.

Although no life data was given, it is conjectured that the bronze pumps will last longer than the fifteen-year solar system life frequently used for analysis.

Table 3.8. Pump Cost

Centrifugal Pumps

HP	Material	Manufacturer	Cost w/o Motor	Cost w/Motor
1/3	Phenolic	Flotec, Inc.		$ 99.00
	Rubber	Simei Pump Co.		44.00
1/2	Bronze	Burks Pumps		232.00
1/2	Bronze	Simei Pumps		390.00
1/2	Iron	Gusher		135.20
1/2	Bronze	Price Pump Co.		190.00
1/2	Bronze	Teel Pump Co.	$ 82.45	121.30

Positive Displacement Pumps

HP	Material	Manufacturer	Cost w/o Motor	Cost w/Motor
1/2	Bronze	Lobee Pump	$ 90.00	$206.00
1/3	Bronze	Flotec, Inc.		$206.00
1/4	Plastic Tube	Randolph Co.	143.00	191.00

ORIGINAL PAGE IS
OF POOR QUALITY

EXPERIMENTAL PROGRAM

A preliminary evaluation of pump performance was initiated to determine the efficiencies of the small pumps indicated in the previous section. First, it was important to see how the centrifugal pump efficiency compared from one manufacturer to another. Then two positive-displacement pumps were tested for a limited comparison to the centrifugal pumps.

The testing program was conducted in two phases. In the first, the evaluation of pump operating characteristics was accomplished using the experimental apparatus shown in Figure 3.1. In the second, the apparatus shown in figure 3.2 was used.

In the first, a constant head tank was maintained by using a large-capacity pump to recirculate water at a higher rate than that delivered by the test pump. An overflow outlet was allowed to maintain this constant head. The mass flow rate through the pump was measured by inserting a bucket between the exit and the lower reservoir to collect a sample and by using a stopwatch to measure the collection period. A root-sum-square error analysis of this measurement system indicated that the error in measuring mass flow rate was less than ±1% for all flow rates tested.

The pressure drop across the pump was measured by using a U-tube manometer for those cases where the head was less than ten psi (68,947.6 Newton/meter^2). The error in measuring pressure was less than ±2.5% for the smallest pressure measurements to ±.5% at the highest heads. When heads were outside the range of the mercury manometer, the inlet pressure was measured using a water manometer and the outlet pressure was measured using a Bourdon tube gage. The error in measuring head with this system was less than ±2.5% at ten psi. At 30 psi, the error was less than ±1% of the reading.

ORIGINAL PAGE IS
OF POOR QUALITY

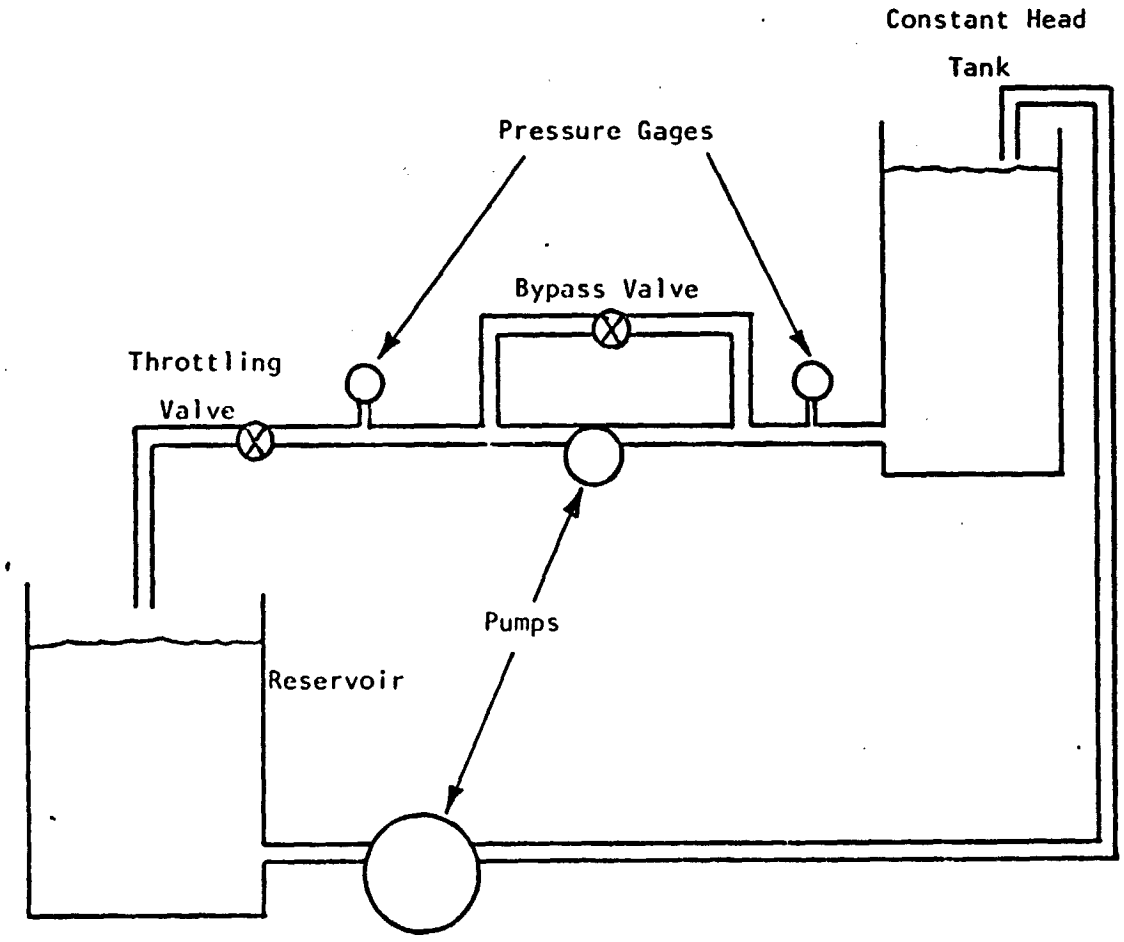

Figure 3.1. Experimental Apparatus for the Smaller Pumps

The electrical power input to the pump was measured using a Weston watt meter which was calibrated. The error in measuring power was less than ±2% for every test except for one magnetic-driven pump which used only 27 watts. For this the error was less than ±5% of actual reading.

A laboratory dynamometer was used to test two of the electric motors which were not directly connected to the pumps evaluated in this study. This unit was specified to be accurate to within ±5%. However, there was no way to calibrate the system with the facilities available.

The scope of the study was extended to include evaluation of the performance of additional pumps, including some larger pumps. For this reason, all instrumentation remained the same, but the test apparatus was modified to maintain a constant head at the higher flow rates. Data collected in the initial tests were all for small pumps of one-third horsepower or less. The second stage of testing started at one-fourth horsepower and included pumps up to one horsepower in size.

Governing Equations Used in the Experimental Study

A summary of the equations used to evaluate the data is presented in this section for reference purposes. This summary is illustrated via a sample calculation.

Sample Calculation

A sample calculation for one experimental point from the 1/4 hp data is presented to indicate the data analysis methods. The data collected were: Mass collected = 117.4 lbm, time of collection = 44.4 seconds, manometer reading (water over mercury) = 9.38 inches, electrical power = 420 watts. All tests were run with water at 66°F. This set of data corresponds to the latter set of tests using the apparatus shown in Figure 3.2.

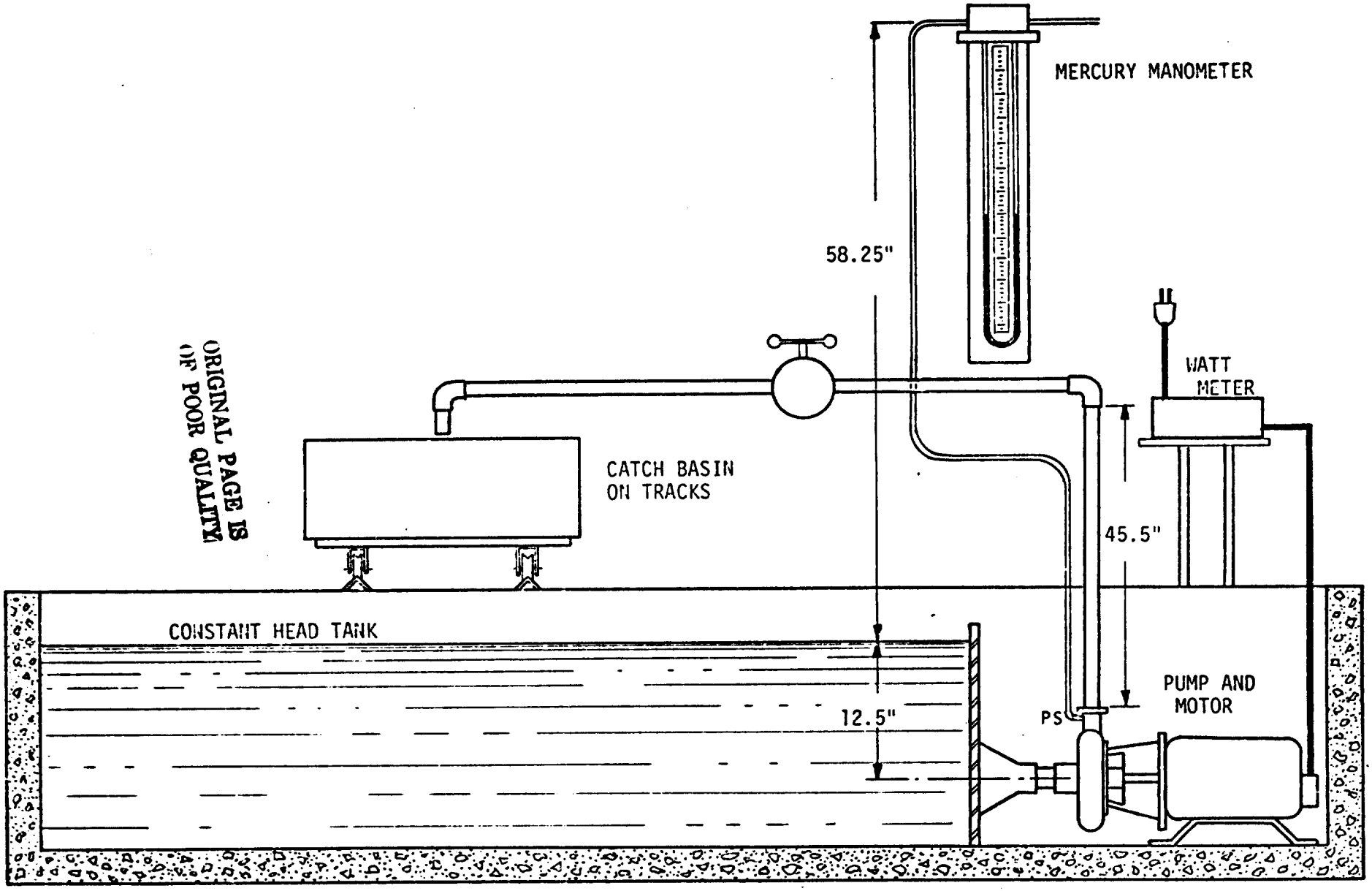

ORIGINAL PAGE IS OF POOR QUALITY

Figure 3.2. Experimental Apparatus for the Second Phase

Mass Flow Rate. M = 117.4 lbm/44.4 seconds = 2.64 lbm/second. With a water temperature of 66°F, the density is 62.31 lbm/ft^3. The volume flow rate is given by

$$Q = \frac{\dot{m}}{\rho} = .0424 \text{ ft}^3/\text{sec} \tag{3.5}$$

$$= .0012 \text{ m}^3/\text{sec}$$

Pressure Differential Across the Pump. The pressure differential across the pump is determined by correcting the manometer reading for static differential, friction loss, and dynamic head of the fluid at the pressure tap.

In Figure 3.2, it can be seen that the static head between the constant head tank and the manometer connection is 58.25 inches of water (ΔP_s = 1.48 meters of water). The friction loss can be found for the inlet to the pump and for the outlet losses to the pressure tap. For this pump it was negligible. The actual inside diameter of 0.825 inches can be used with the volume flow rate to determine the average fluid velocity

$$V = \frac{\dot{Q}}{A} = \frac{(.0424)(144)}{(\pi/4)(.825)^2} \text{ ft/sec} \tag{3.6}$$

$$= 11.42 \text{ ft/sec} = 3.481 \text{ m/sec}$$

The dynamic head is given by

$$\Delta H_d = \frac{1}{2} \rho \frac{V^2}{g_c} = \frac{(62.31)(11.42)^2}{(64.4)(144)} = 0.88 \text{ psi} \tag{3.7}$$

$$= 0.62 \text{ meters of water}$$

The manometer reading is for water over mercury. Therefore, the pressure difference is

$$\Delta p_m = \rho \frac{g}{g_c} (12.6) h =$$

$$= \frac{(62.31)}{144} \left(\frac{32.14}{32.17}\right)(12.6)\left(\frac{9.38}{12}\right) = 4.26 \text{ psi} \tag{3.8}$$

which is equivalent to

3.00 meters of water

ORIGINAL PAGE IS
OF POOR QUALITY

For the particular sample data point the total head imposed on the pump is

$$\Delta H = \Delta H_s + \Delta H_d + \Delta H_m \tag{3.9}$$

$$= 1.48 + .62 + 3.00 = 5.1 \text{ meters of water}$$

Water Power

The water power produced by the pump is given by

$$WHP = \dot{Q}\Delta H(9.306 \times 10^{3}) \tag{3.10}$$

$$= 60.01 \text{ watt}$$

Overall Efficiency

The overall efficiency is the water power divided by the electrical power input. This is given by

$$\eta_o = \frac{WHP(100)}{EP} = \frac{60.01(100)}{420} = 14.3\% \tag{3.11}$$

RESULTS

Initial Tests

In the initial set of tests, five centrifugal pumps and two positive displacement pumps were tested. Two of the centrifugal pumps were magnetically driven; consequently, it was not possible to separately test the electric motor driving them. Two of the centrifugal pumps and one of the positive displacement pumps were directly mounted to the motor shaft and, likewise, it was not possible to separately evaluate these motors. However, one positive displacement pump and one centrifugal pump involved independent units. The motors for these two were tested. Table 3.9 summarizes the pumps tested in the initial phase. Figure numbers for the corresponding results are listed for reference.

Table 3.9. Summary of Pumps Tested in Initial Set of Tests

Pump	Type	Figure Number(s) of Results
Magnetically Driven Teel, 1/20 hp	Centrifugal	3.3
Magnetically Driven March, 1/12 hp	Centrifugal	3.4
Directly Coupled Flotec 1/4 hp	Centrifugal	3.5
Directly Coupled Fastern 1/4 hp	Centrifugal	3.6
Bell Driven Teel, 1/4 hp	Centrifugal	3.7
Teel, 1/3 hp	Positive Displacement	3.8, 3.9
Flotec, 1/3 hp	Positive Displacement	3.10

The water power for all pumps in the initial set of tests was calculated using the expression $hp = \dot{Q}\Delta P$. Using this equation and the measured input power, an error analysis of the efficiency for each pump was found to be less than ±6%. This analysis was based on data given in the experimental section of this report. A root-sum-square error analysis was used. The percent error is found by

ORIGINAL PAGE IS OF POOR QUALITY

$$\frac{\Delta\eta}{\eta}\Big|_{rss} = \sqrt{\left(\frac{\Delta\dot{Q}}{\dot{Q}}\right)^2 + \left(\frac{\Delta P}{P}\right)^2 + \left(\frac{\Delta EHP}{EHP}\right)^2} \qquad (3.12)$$

where η = calculated efficiency = hp/EHP,

EHP = electrical power measurement.

Since all pumps are rated in gallons per minute and head in feet of water, these units are shown on the figures.

Figure 3.3 gives the data for Teel model 1P760 magnetic drive pump of low-flow capacity. Figure 3.4 gives the data for the March MPX-3 magnetic drive pump. These were the only pumps tested which were not in the 1/4-1/3 hp range. A water manometer was used for these tests to measure the pressure head across the pump.

Figures 3.5 and 3.6 show results for the centrifugal pumps with attached motors.

Before the data for the last centrifugal pump tested in the first phase are presented, results of the efficiency tests for two of the electric motors are presented. The experimental results are tabulated in Table 3.10.

Table 3.10. Electric Motor Efficiencies

Pump Rating, HP	Power Input, watts	Power Output, watts	η_e, %
1/4, Wagner	275	77.2	28
1/4, Wagner	325	97.7	30
1/4, Wagner	440	185.5	42.2
1/4, Wagner	700	338.5	48.4
1/3, Leland Faraday	225	88.0	39.2
1/3, Leland Faraday	330	149.0	45.2
1/3, Leland Faraday	375	215.3	57.4
1/3, Leland Faraday	425	246.9	58.1
1/3, Leland Faraday	500	276.5	55.3

The efficiency of the 1/4 hp motor at a rated output of 1/4 hp was 42.2%. The efficiency of the 1/3 hp motor at the rated output of 1/3 hp was about 58%. The efficiencies shown in Table 3.10 can be used for the actual power consumed in

Figure 3.3. Teel 1P760 Centrifugal Pump, Magnetic Drive

ORIGINAL PAGE IS
OF POOR QUALITY

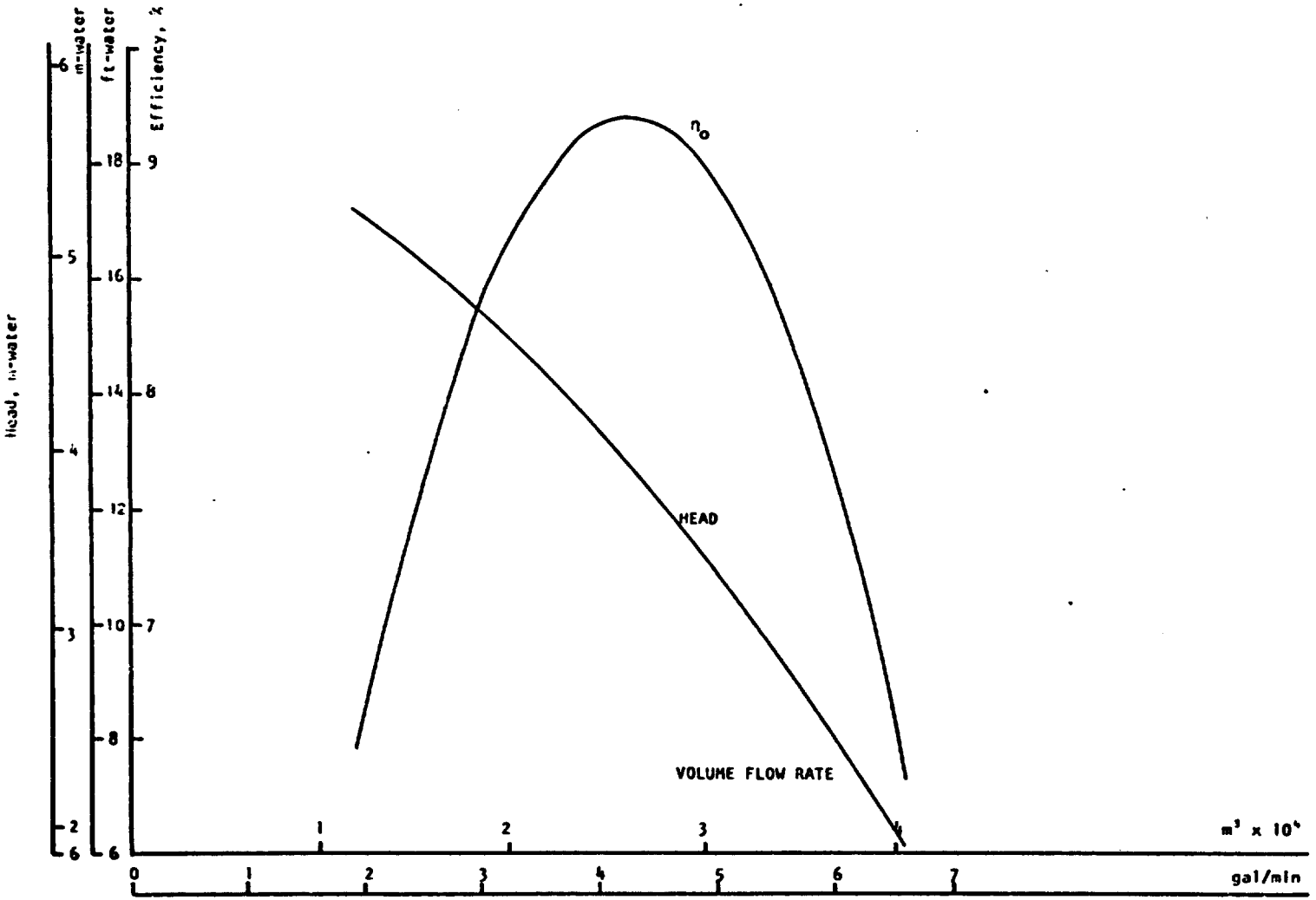

Figure 3.4. March Centrifugal Pump MPX-3

ORIGINAL PAGE IS
OF POOR QUALITY

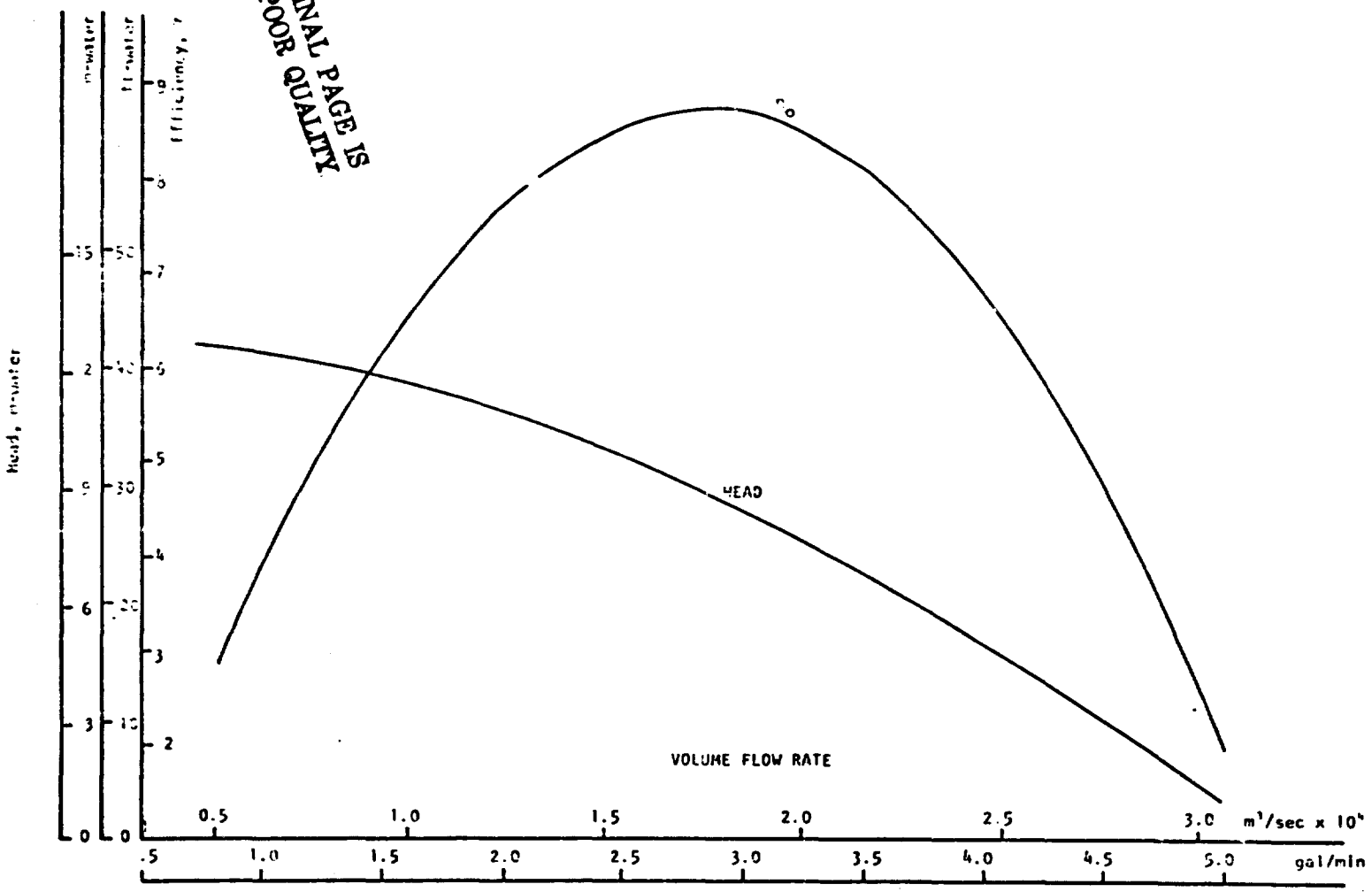

Figure 3.5. . Flotec 1/4 hp Centrifugal Pump

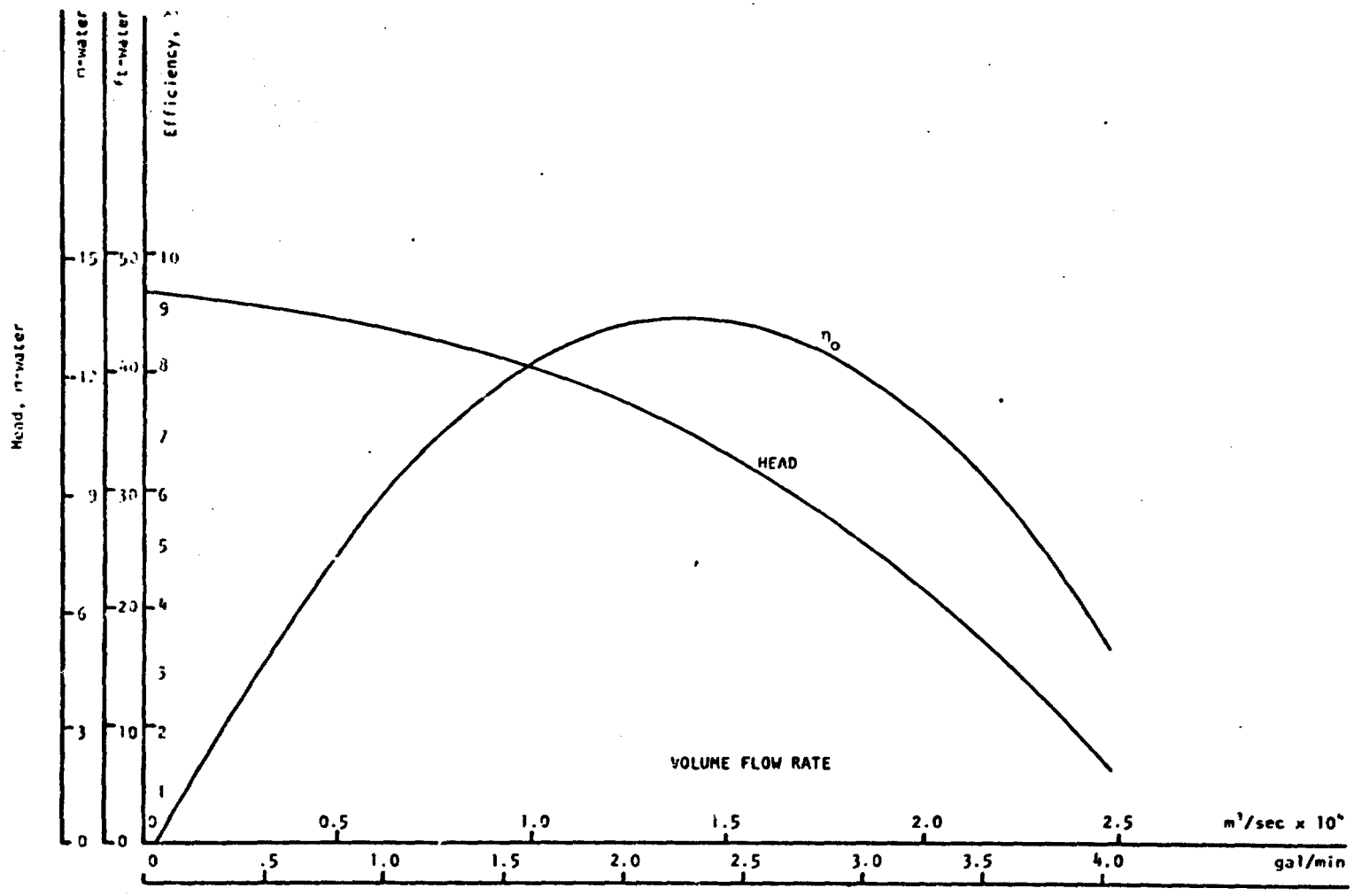

Figure 3.6. Eastern 1/4 hp Centrifugal Pump

the pump tests to approximate the pump efficiencies at each test point by dividing the overall efficiency η_o, by the electric motor efficiency η_e. The resulting efficiency is called the pump efficiency, η_p.

$$\eta_p = \eta_o/\eta_e \tag{3.38}$$

Strictly speaking, η_p calculated in this manner includes the coupling efficiency.

Figure 3.7 shows plots of overall efficiency and pump efficiency for four different shaft rotational speeds for the teel centrifugal pump that was belt driven. The head characteristics are not shown to avoid confusion.

Figures 3.8 and 3.9 show results for flow control by throttling and by-pass techniques, respectively, using the same positive displacement pump. Variation in rotational speed was not plotted.

A Flotec positive displacement pump with adjustable capacity was also tested. This particular pump had a mechanical adjustment which made it possible to reverse the flow when the lever was located below the pump centerline. The results are shown in Figure 3.10. The motor was not independently tested and only values of overall efficiency were obtained.

Final Testing Program

The results of the initial testing program indicated that small pumping systems had an overall efficiency which was much less than was expected. The effect of the electric motor efficiency coupled with the low efficiency of the small pumps gave an overall efficiency, in many cases, which was less than ten percent for the small pumps.

One of the objects of the final phase of testing was to test a complete line of pumps from one manufacturer in an effort to evaluate a typical performance spectrum over a range of sizes. The complete line tested included 1/4, 1/3, 1/2, 3/4 and 1 horsepower pumps. The Bell and Gossett manufactured pumps were selected for these tests. Then, three other commonly-used centrifugal

ORIGINAL PAGE IS

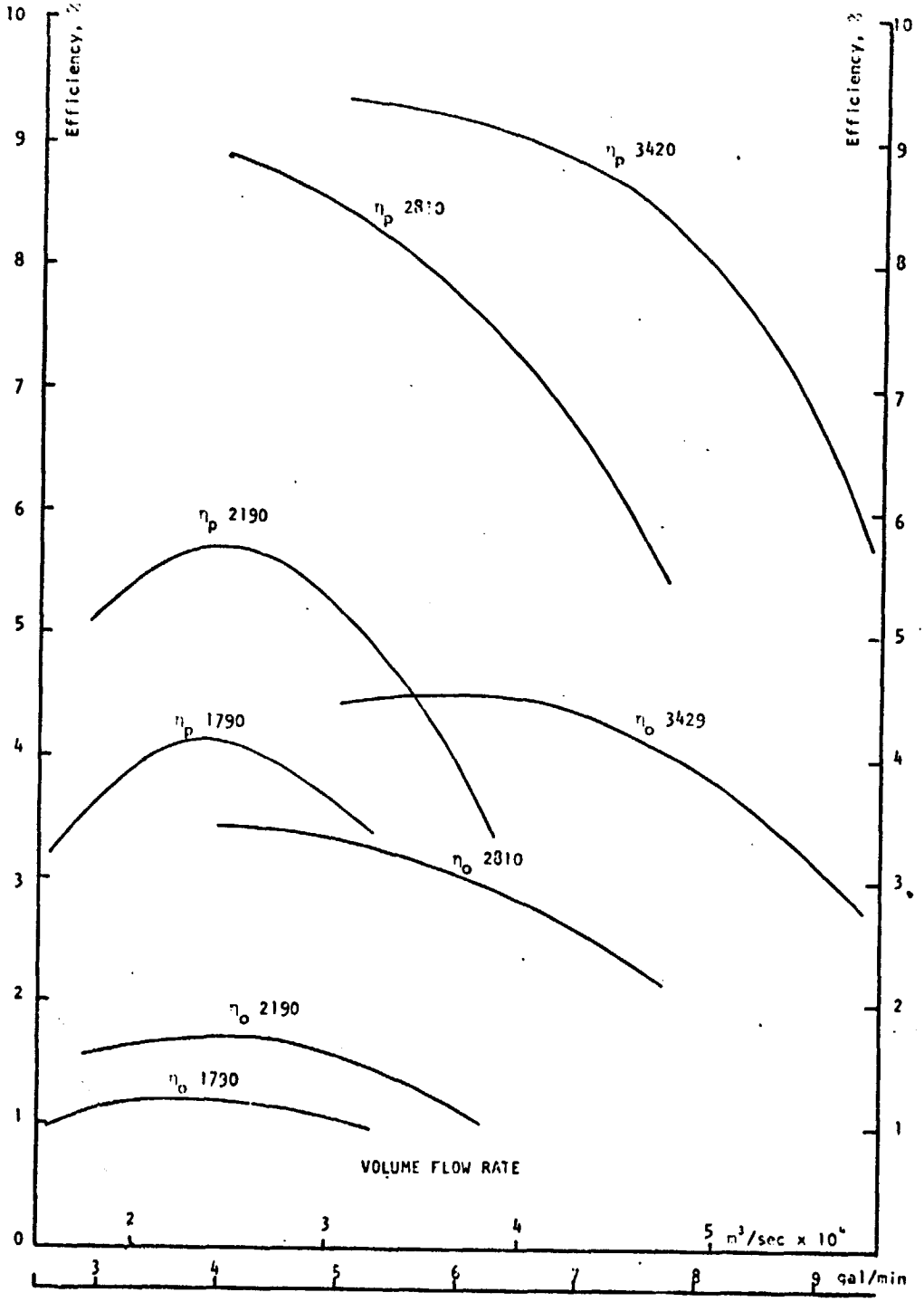

Figure 3.7. Rotations Speed Effect on Efficiency of Teel Pump

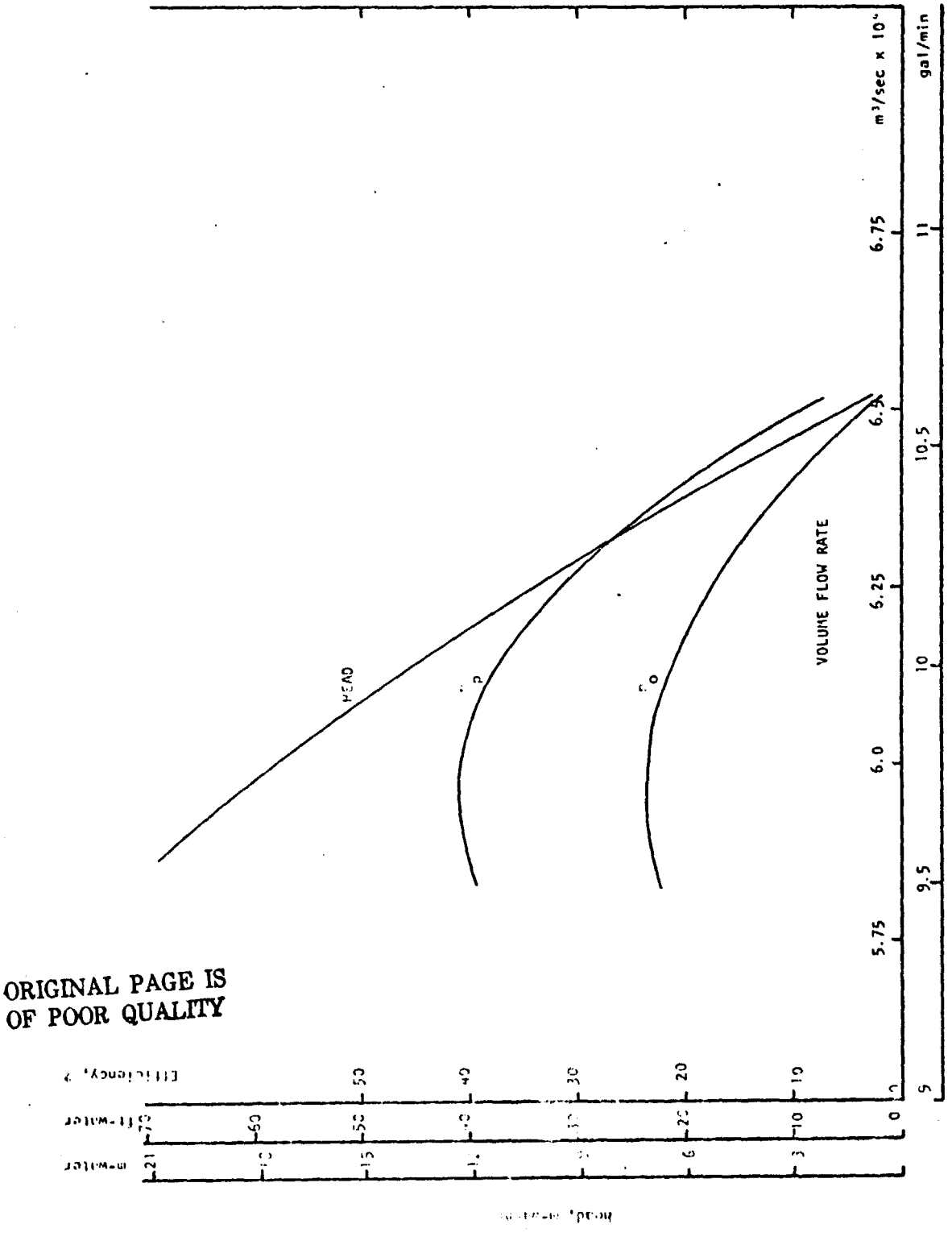

Figure 3.8. Teel Gear Pump-Throttle Valve Control

ORIGINAL PAGE IS
OF POOR QUALITY

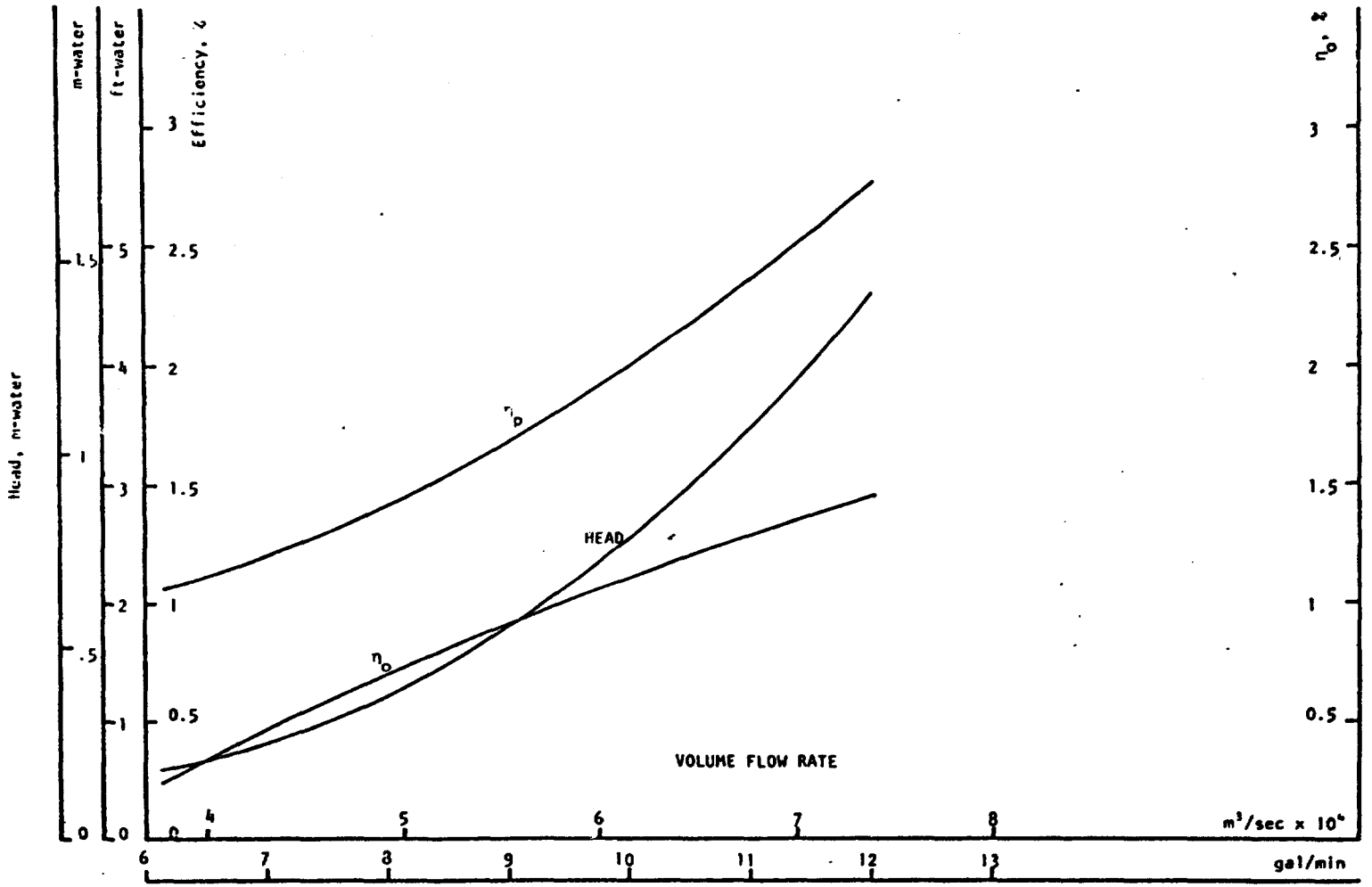

Figure 3.9. Teel Gear Pump By-Pass Control

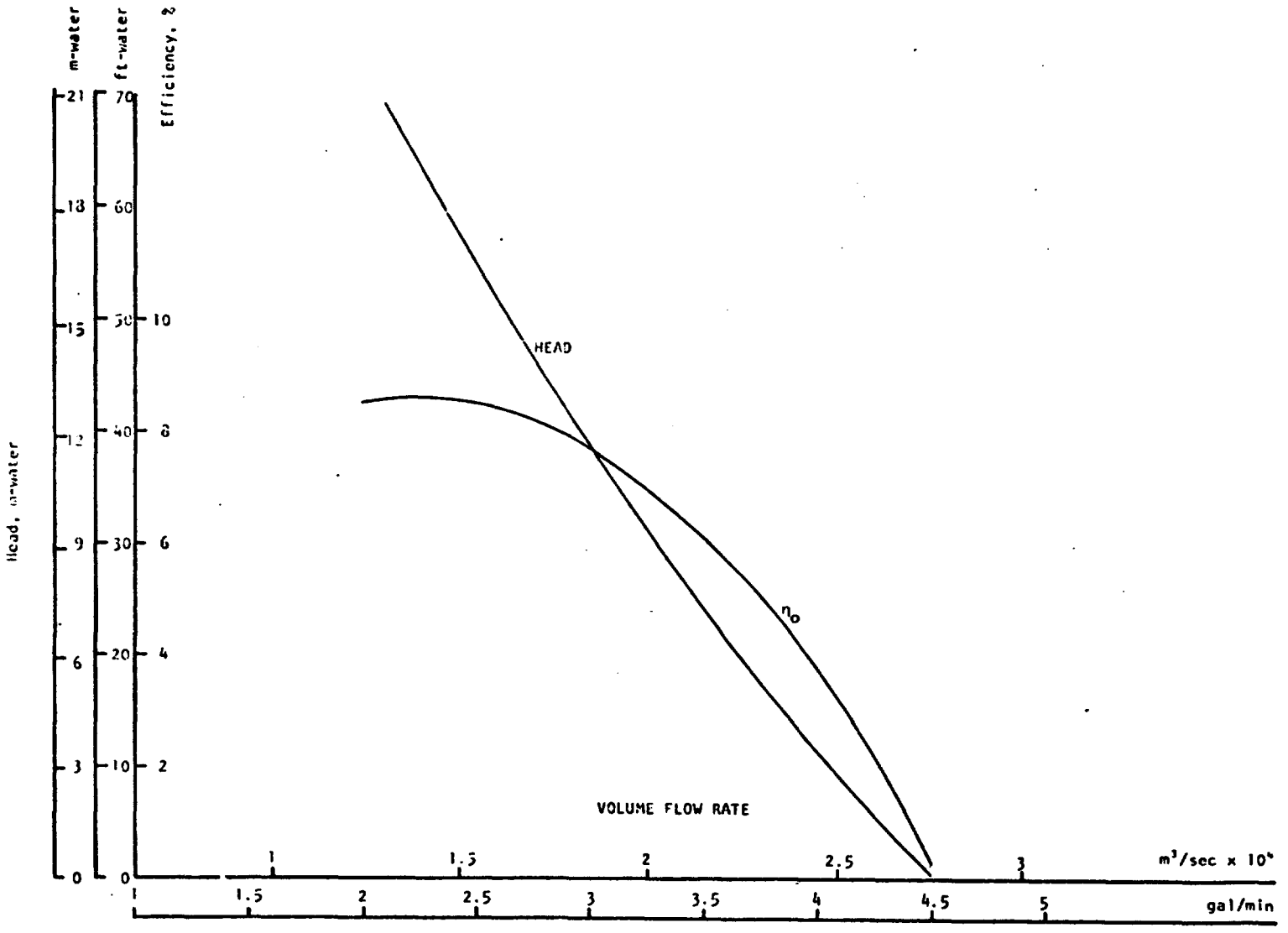

Figure 3.10. Flotec Positive Displacement Pump

ORIGINAL PAGE IS
OF POOR QUALITY

pumps manufactured by three other companies were tested to compare the performance of equal-sized pumps from different suppliers. The three manufacturers were Taco, Myers, and Burk. These were all 1/3 horsepower pumps. Because of the prominence of the Grundfos pumps in a number of solar applications, a 1/12 horsepower of this type was also tested. Finally, two additional 1/3 horsepower positive displacement pumps were tested to be compared with the Teel and Flotec positive displacement pumps which were tested in the initial phase of tests. The Brown and Sharp and the Oberdorfer pumps were selected for these tests. A tabulation of the pumps tested in the final phase of tests is given in Table 3.11.

For these tests, both the overall efficiency and the electric motor efficiency were measured whenever possible. Some pumps were attached to the motor in such a way that separate motor testing was not feasible. (The Grundfos pump is an example of this condition.) The electric motor testing was accomplished using the same power measuring system that was used in the overall efficiency tests. Loads were applied using a dynamometer which could test up to 3/4 horsepower motors.

Each pump was tested by restricting the flow rate up to no flow and then increasing the flow to the lowest possible flow resistance. This process was repeated until approximately one hundred and twenty data points were available for each pump. The actual data points are presented for only two pumps (figure 3.11 and 3.16). The solid curves shown in all cases represent least squares second-order curve fit of the test data. Only the least squared curves were presented for all other pumps.

Performance data for the complete line of Bell and Gossett pumps which were tested are shown in Figures 3.11 through 3.15. Data for the Myers, Taco, Burk and Grundfos pumps are shown, respectively, in Figures 3.16, 3.17, 3.18 and 3.19. For the Brown and Sharpe and Oberdorfer positive-displacement pumps,

the data are shown, respectively, in Figures 3.20 and 3.21. For completeness the data for the Teel and Flotec positive-displacement pumps are shown, respectively, in Figures 3.22 and 3.23.

Table 3.11. Tabulation of Pumps Tested in Final Set of Tests

Size	Type	Manufacturer	Figure Number(s) Showing Results of Tests
1/4 HP	Centrifugal	Bell & Gossett	3.11
1/3 HP	Centrifugal	Bell & Gossett	3.12
1/2 HP	Centrifugal	Bell & Gossett	3.13
3/4 HP	Centrifugal	Bell & Gossett	3.14
1 HP	Centrifugal	Bell & Gossett	3.15
1/3 HP	Centrifugal	Myers	3.16
1/3 HP	Centrifugal	Taco	3.17
1/3 HP	Centrifugal	Burk	3.18
185 w	Centrifugal	Grundfos	3.19
1/3 HP	Positive Displacement	Brown & Sharpe	3.20
1/3 HP	Positive Displacement	Oberdorfer	3.21

Most states have regulations on the noise level which is acceptable for occupied spaces. These were selected to protect those who will be in the space. One list of permissible noise exposure levels is tabulated in Table A.1 in the appendix. Based on the requirements listed there, the sound level at the point of exposure should be below 90 dBA. In an effort to meet these requirements, all pumps in phase two were tested for noise level generation in an effort to indicate their suitability for residential use where continuous occupation is expected. For the noise measurements performed in this work, all measurements were made at a distance of approximately one inch from the source. Since it is unlikely that the point of actual exposure would be of this level, the measurements should be considered conservative and can be compared to the permissible exposure levels listed in the appendix.

ORIGINAL PAGE IS
OF POOR QUALITY

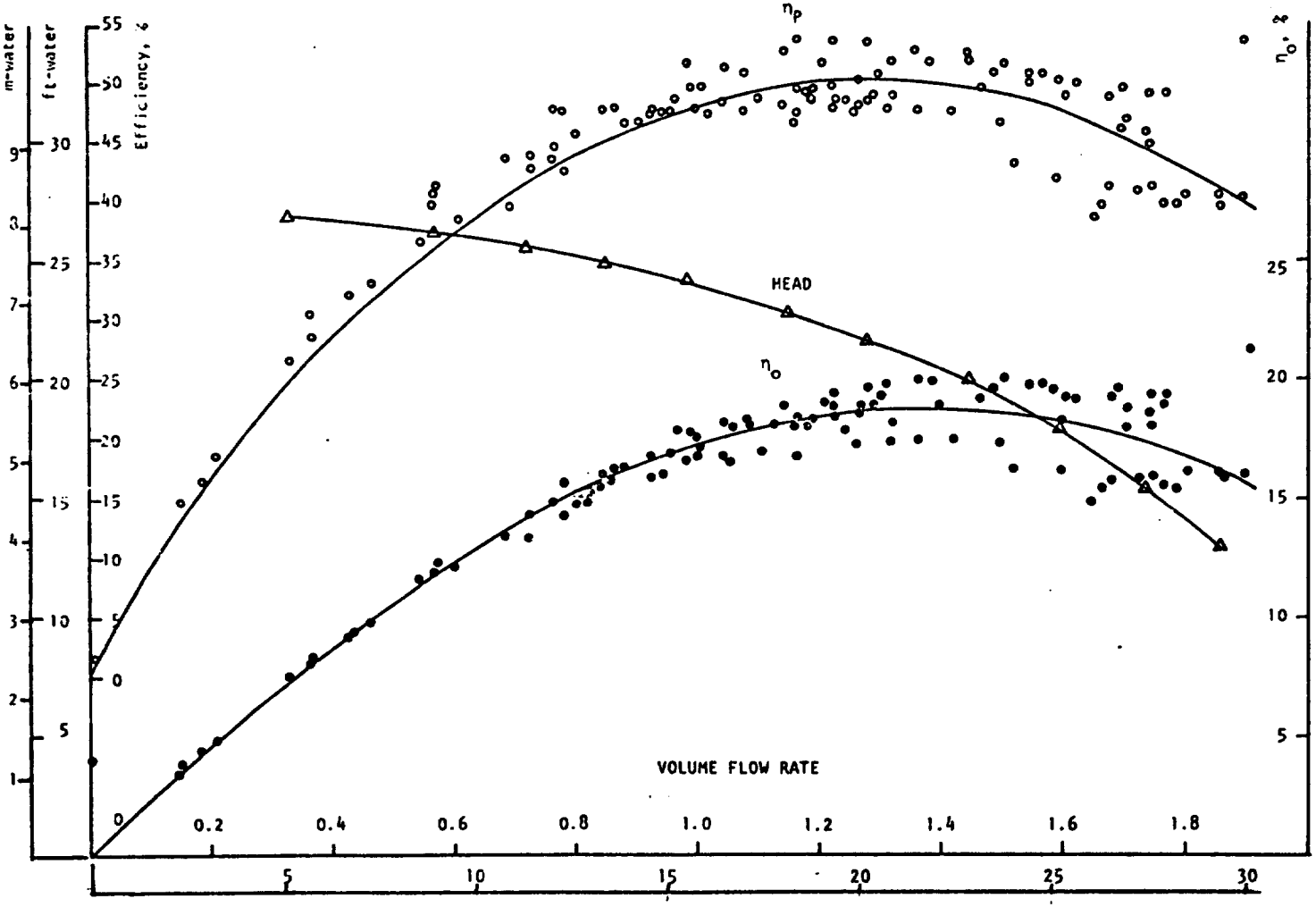

Figure 3.11. Performance Data for 1/4 hp (Bell and Gossett)

ORIGINAL PAGE IS
OF POOR QUALITY

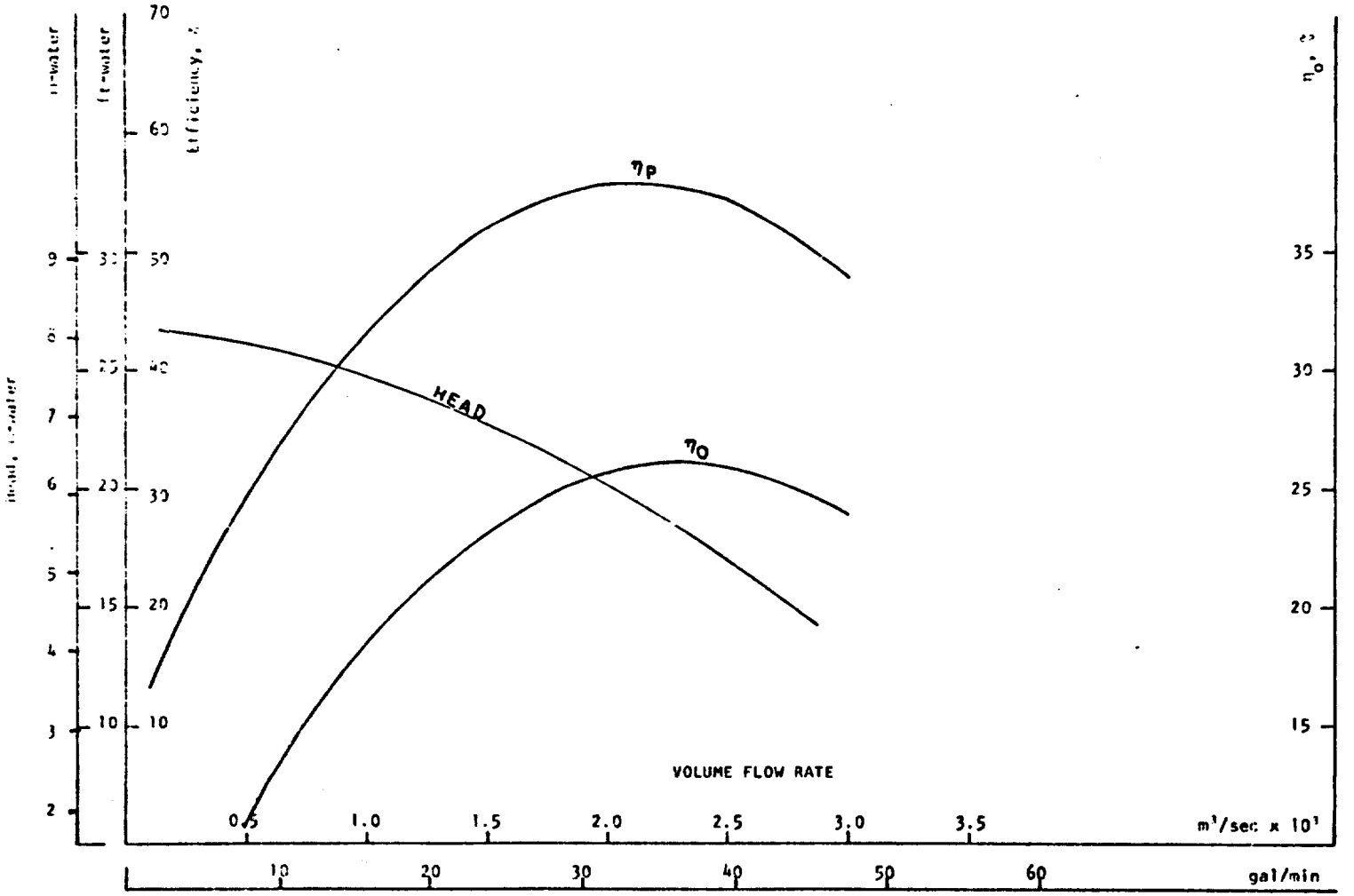

Figure 3.12. Performance Data for 1/3 hp (Bell and Gossett)

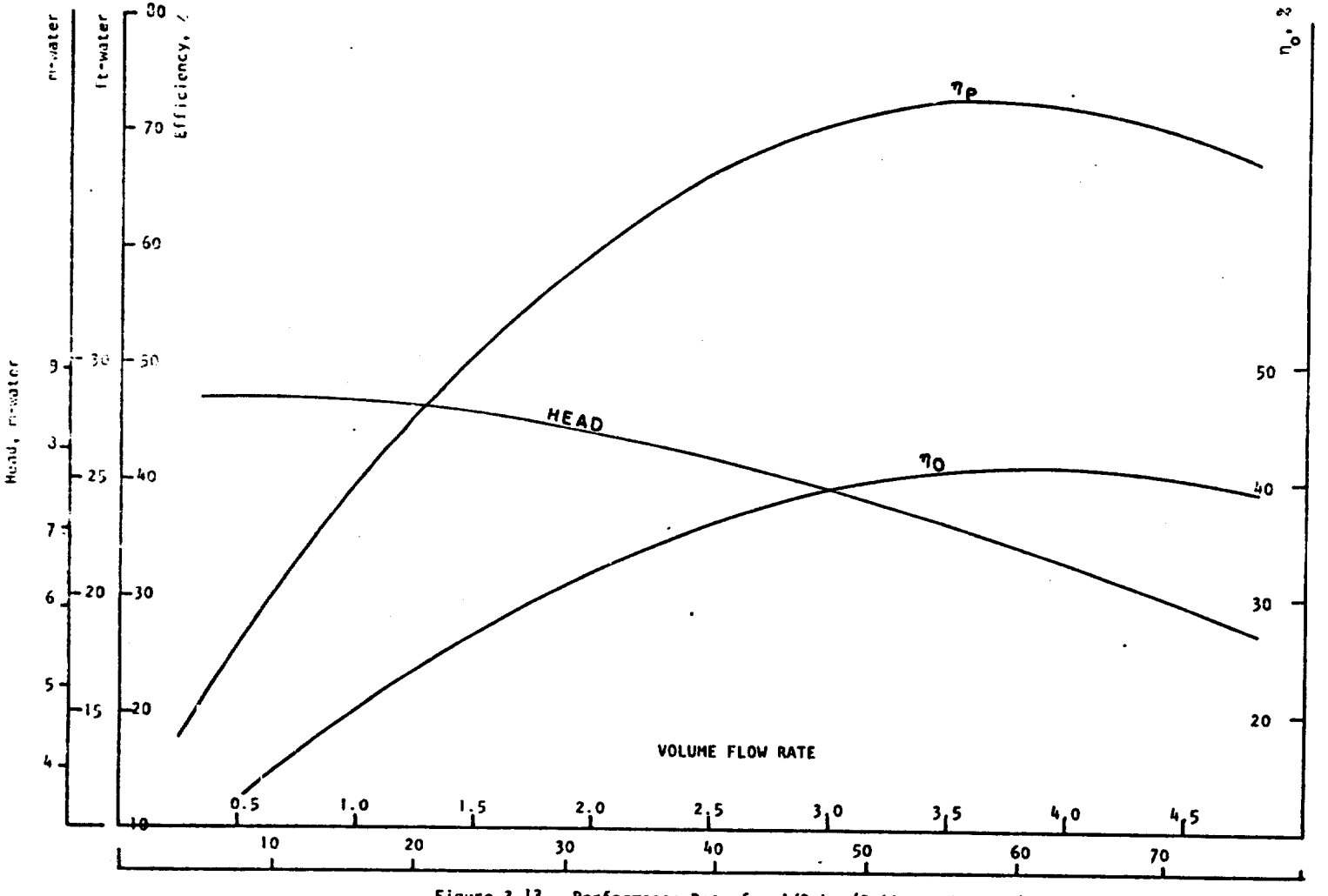

Figure 3.13. Performance Data for 1/2 hp (Bell and Gossett)

ORIGINAL PAGE IS
OF POOR QUALITY

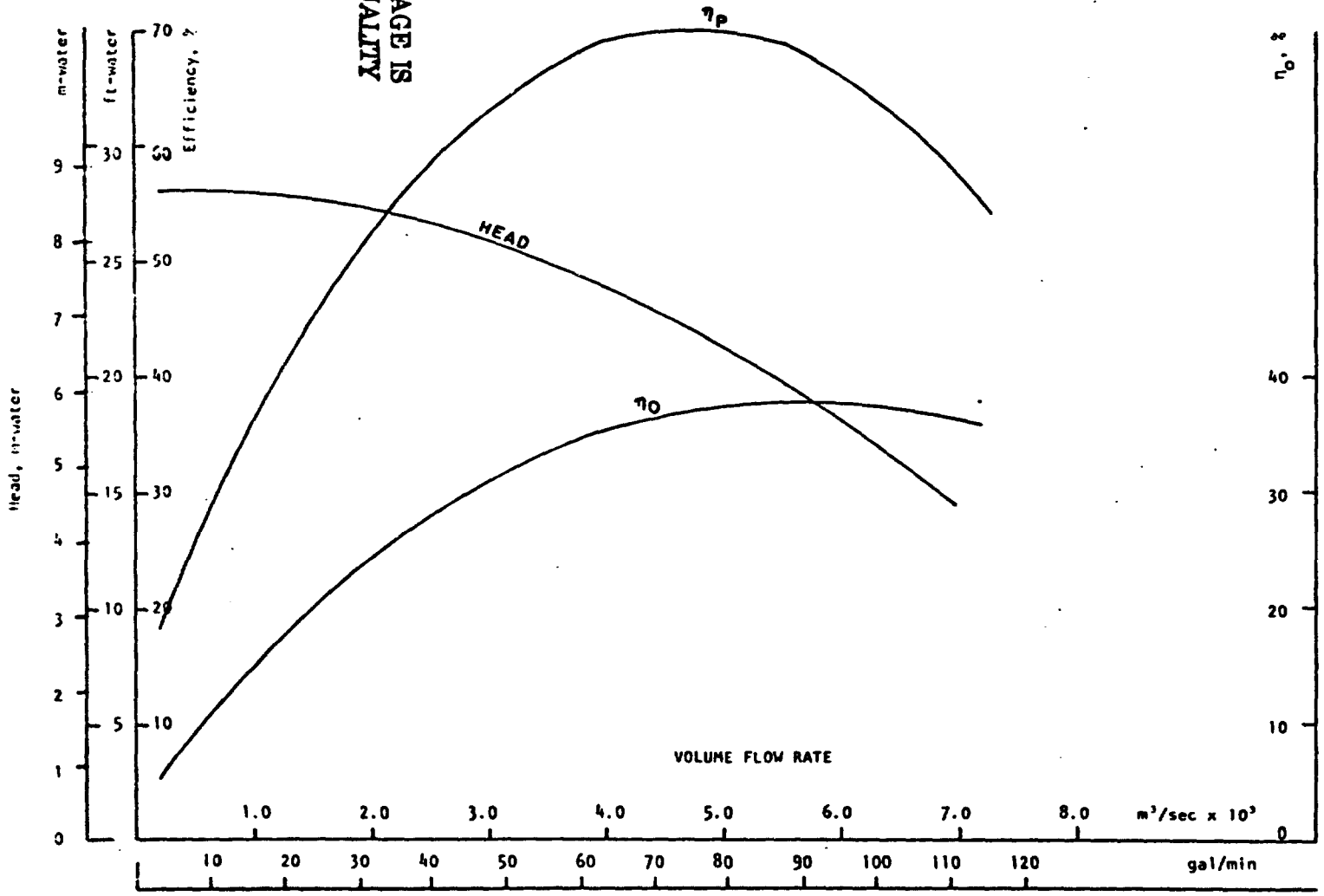

Figure 3.14. Performance Data for 3/4 hp (Bell and Gossett)

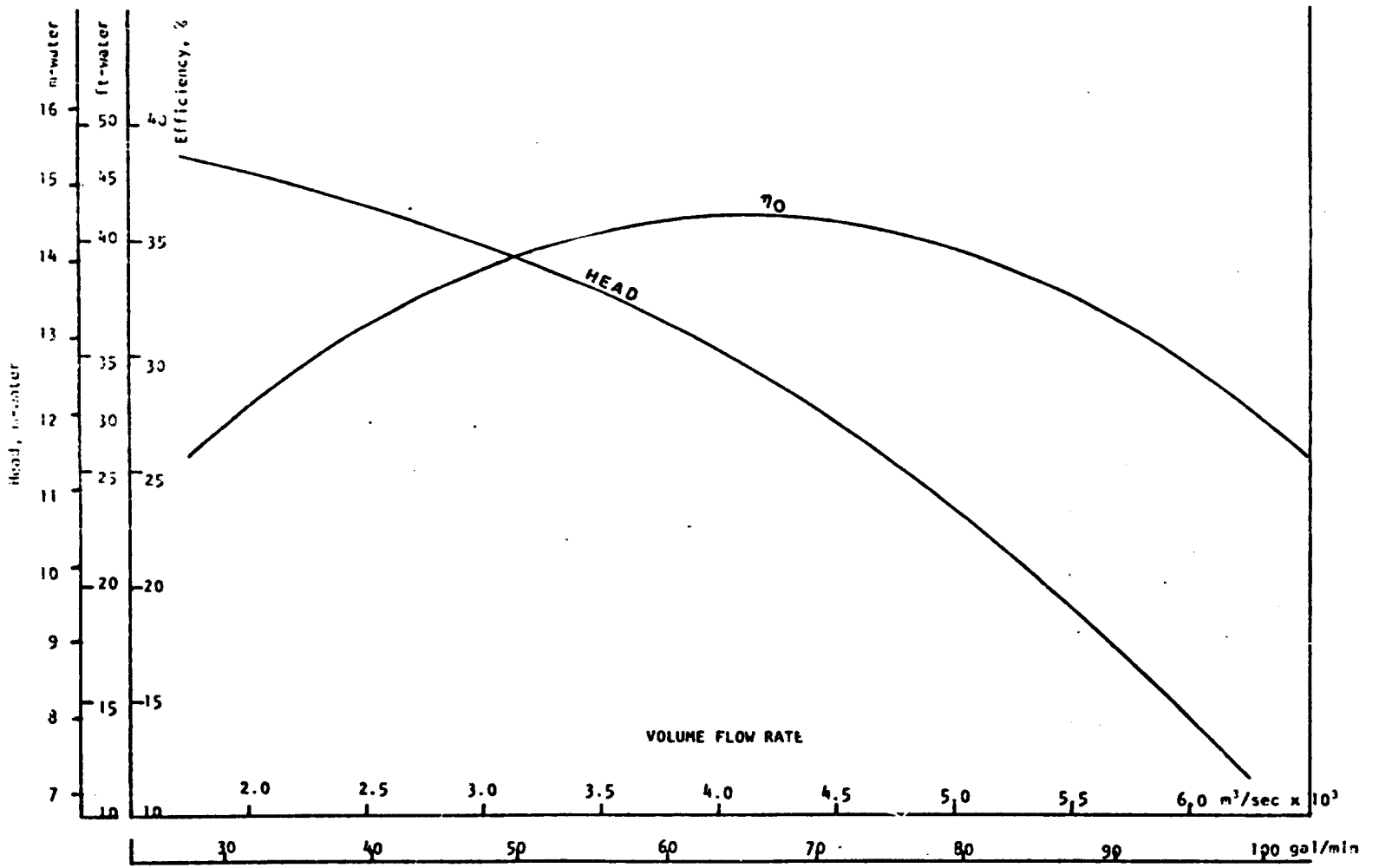

Figur. 3.15. Performance Data for 1 hp (Bell and Gossett)

ORIGINAL PAGE IS
OF POOR QUALITY

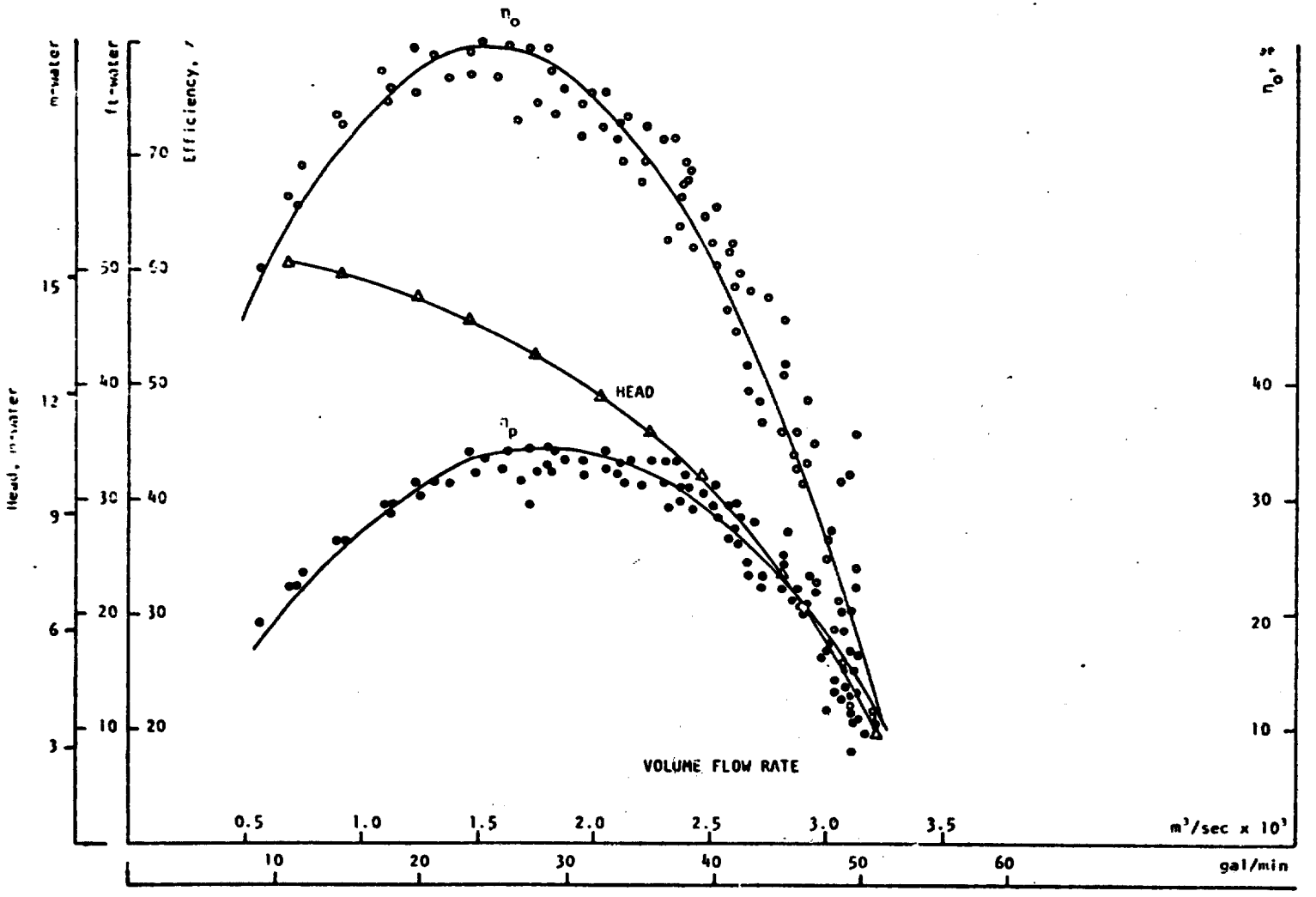

Figure 3.16. Performance Data for 1/3 hp Myers Pump

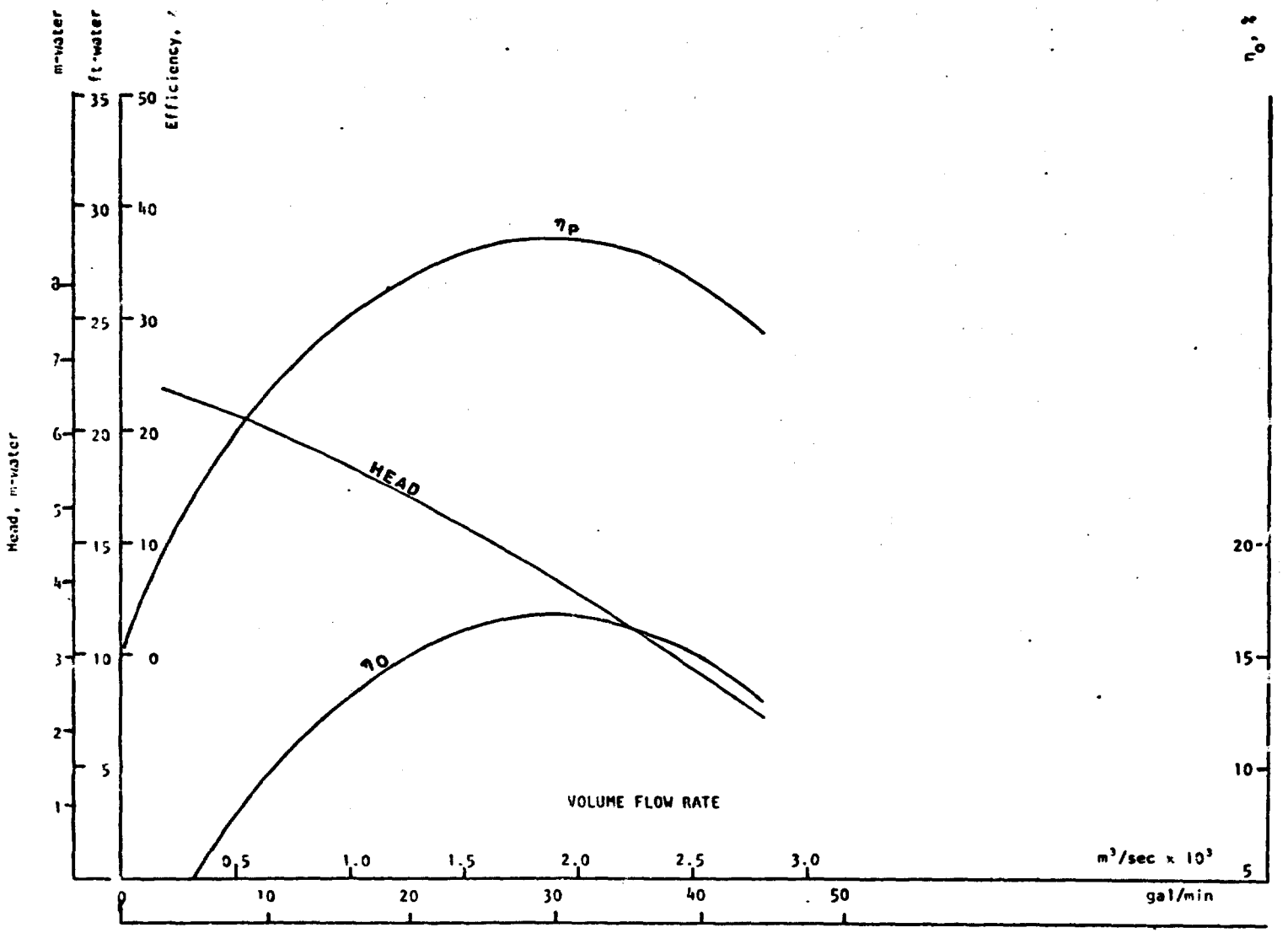

Figure 3.17. Performance Data for 1/3 hp (Taco)

ORIGINAL PAGE IS
OF POOR QUALITY

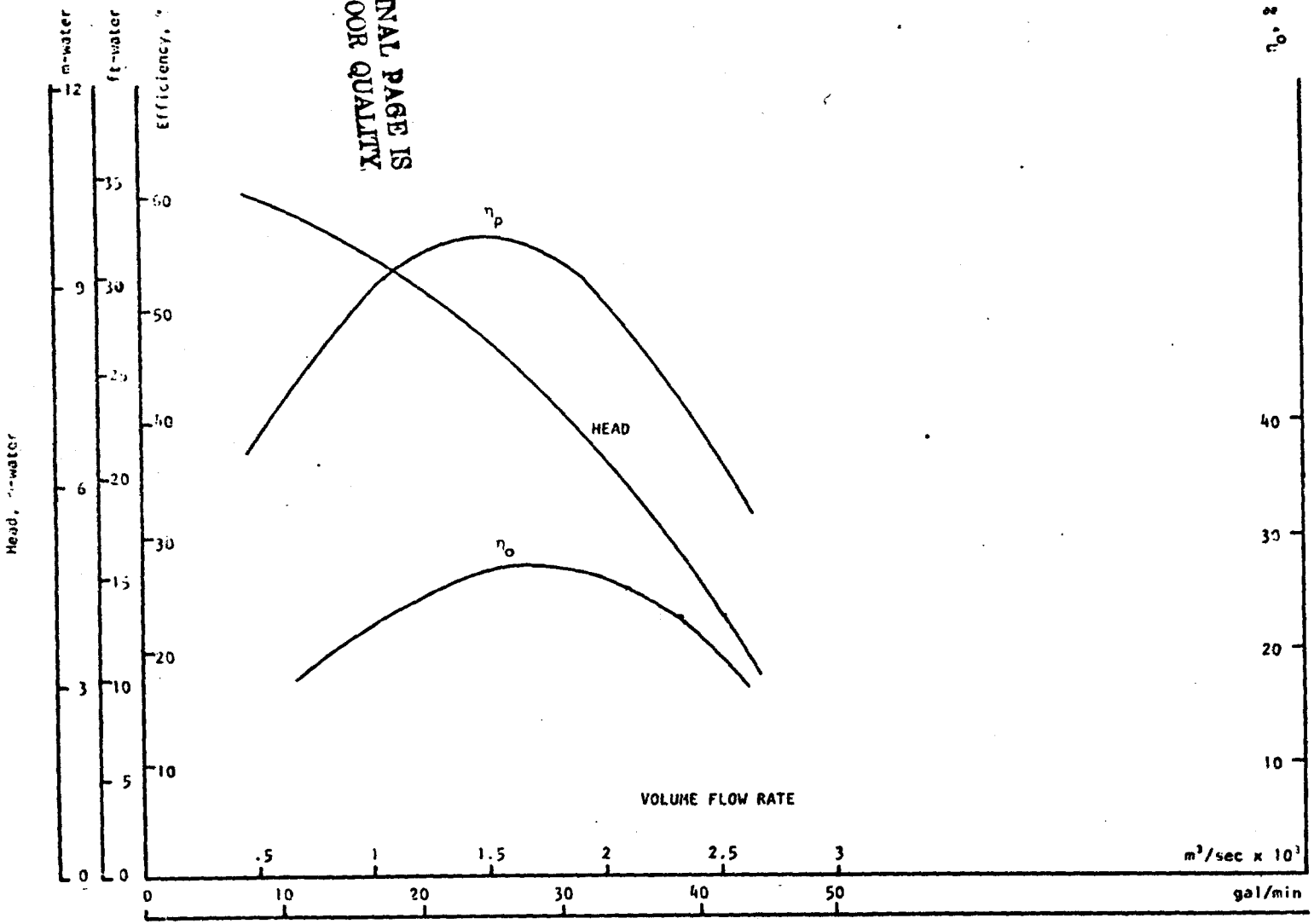

Figure 3.18. Performance Data for 1/3 hp Burk Pump

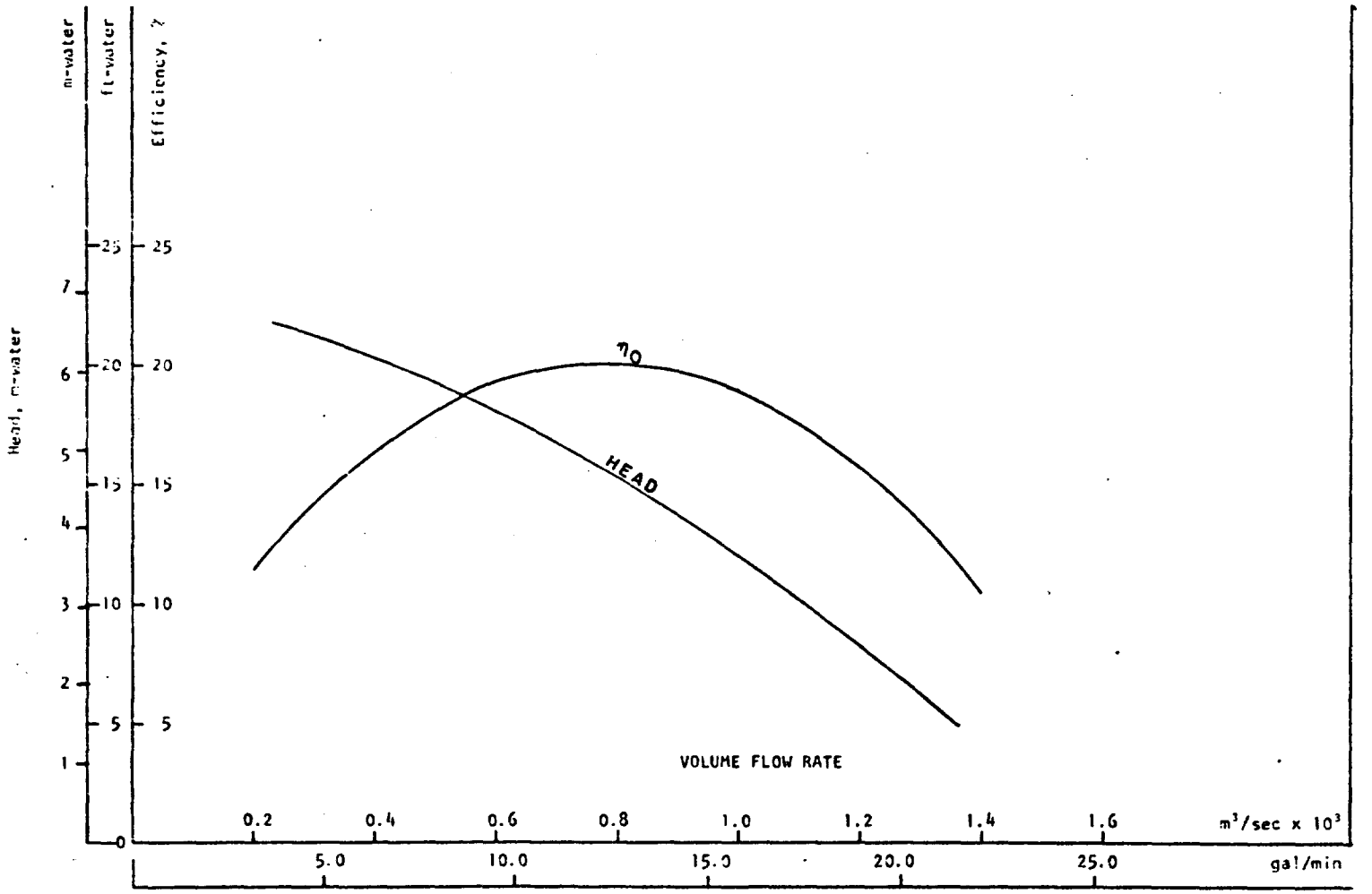

Figure 3.19. Performance Data for 185 w Grundfos Pump

ORIGINAL PAGE IS
OF POOR QUALITY

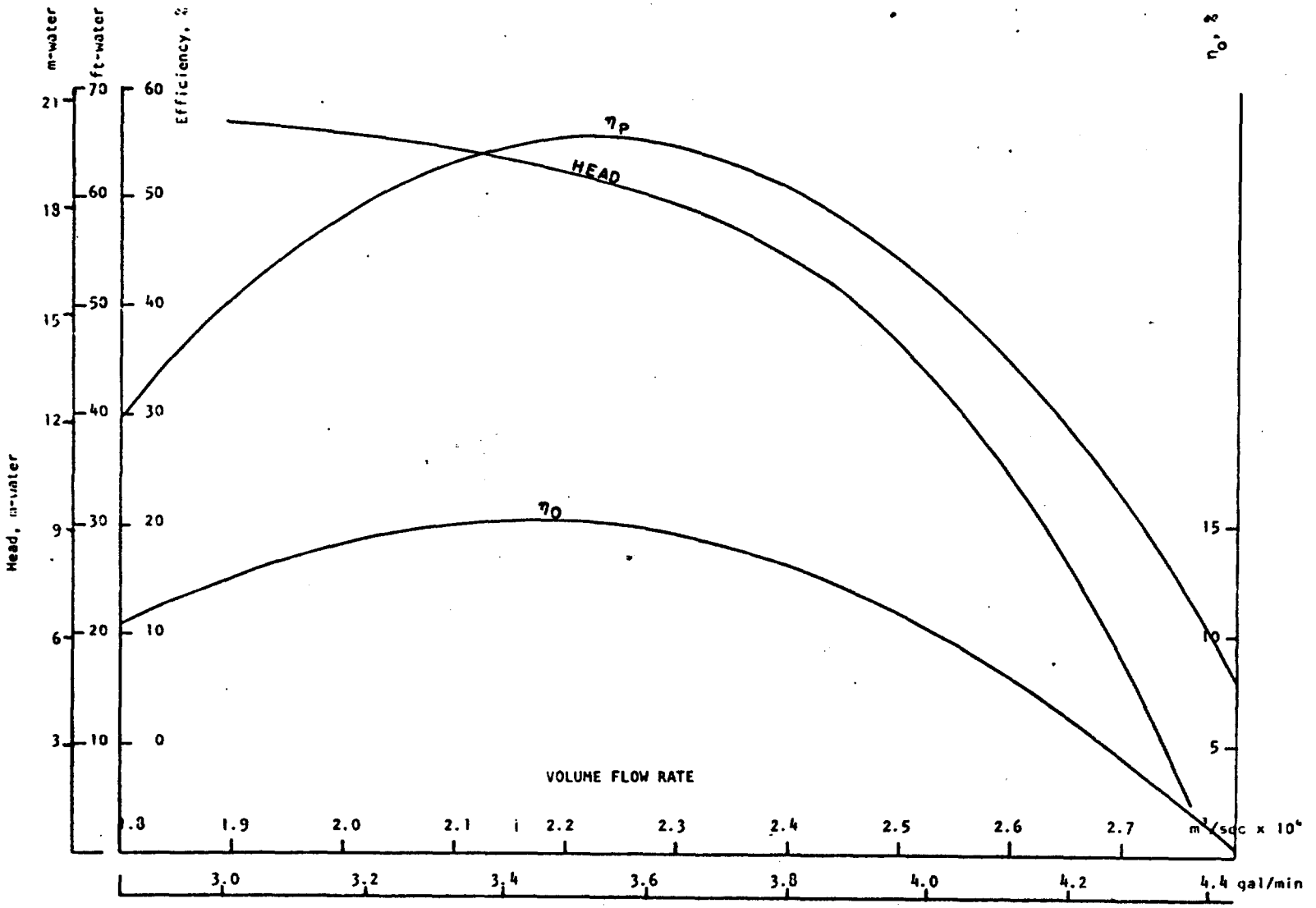

Figure 3.20. Performance Data for 1/3 hp Brown and Sharpe Pump

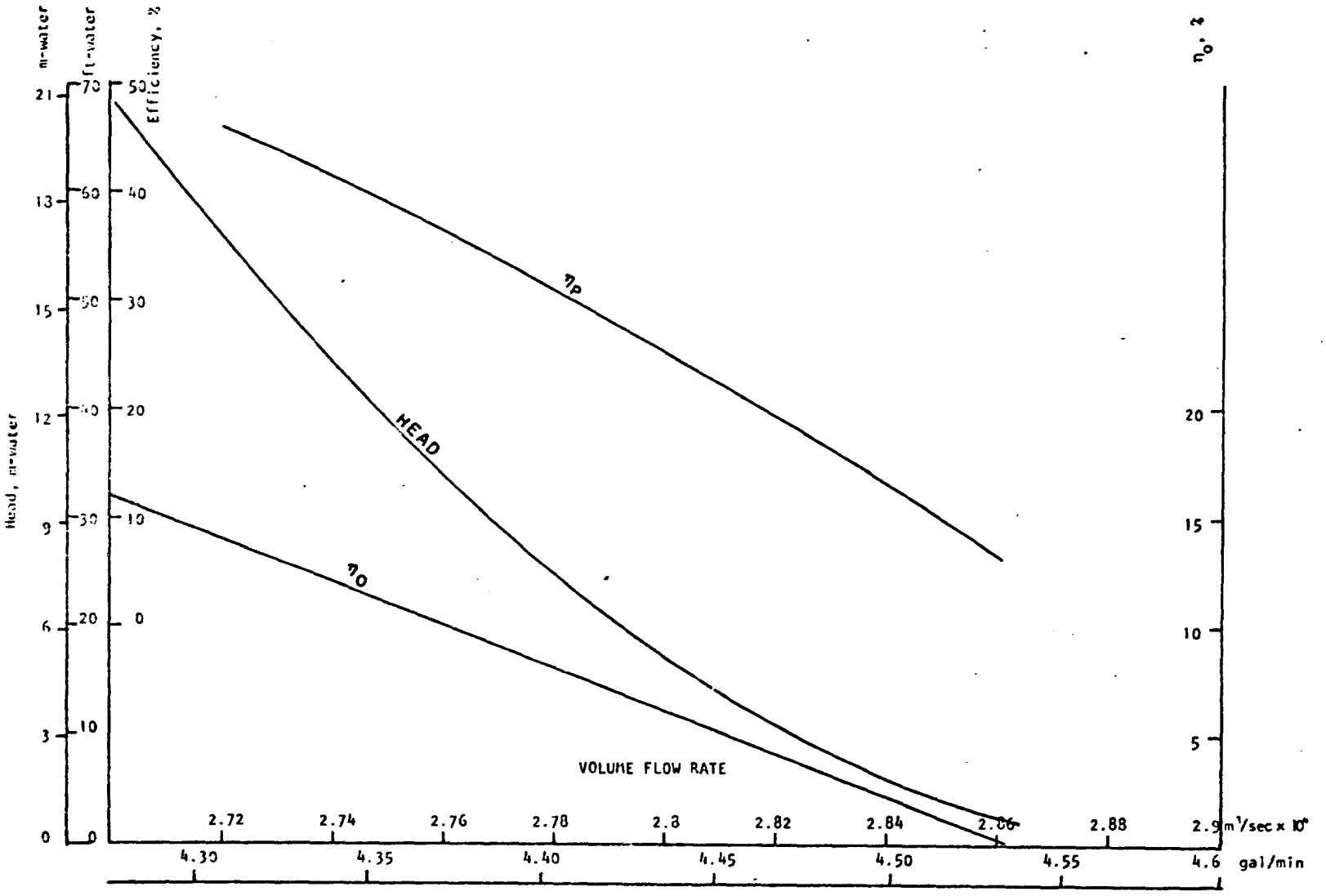

Figure 3.21. Performance Data for 1/3 hp Oberdorf Pump

ORIGINAL PAGE IS
OF POOR QUALITY

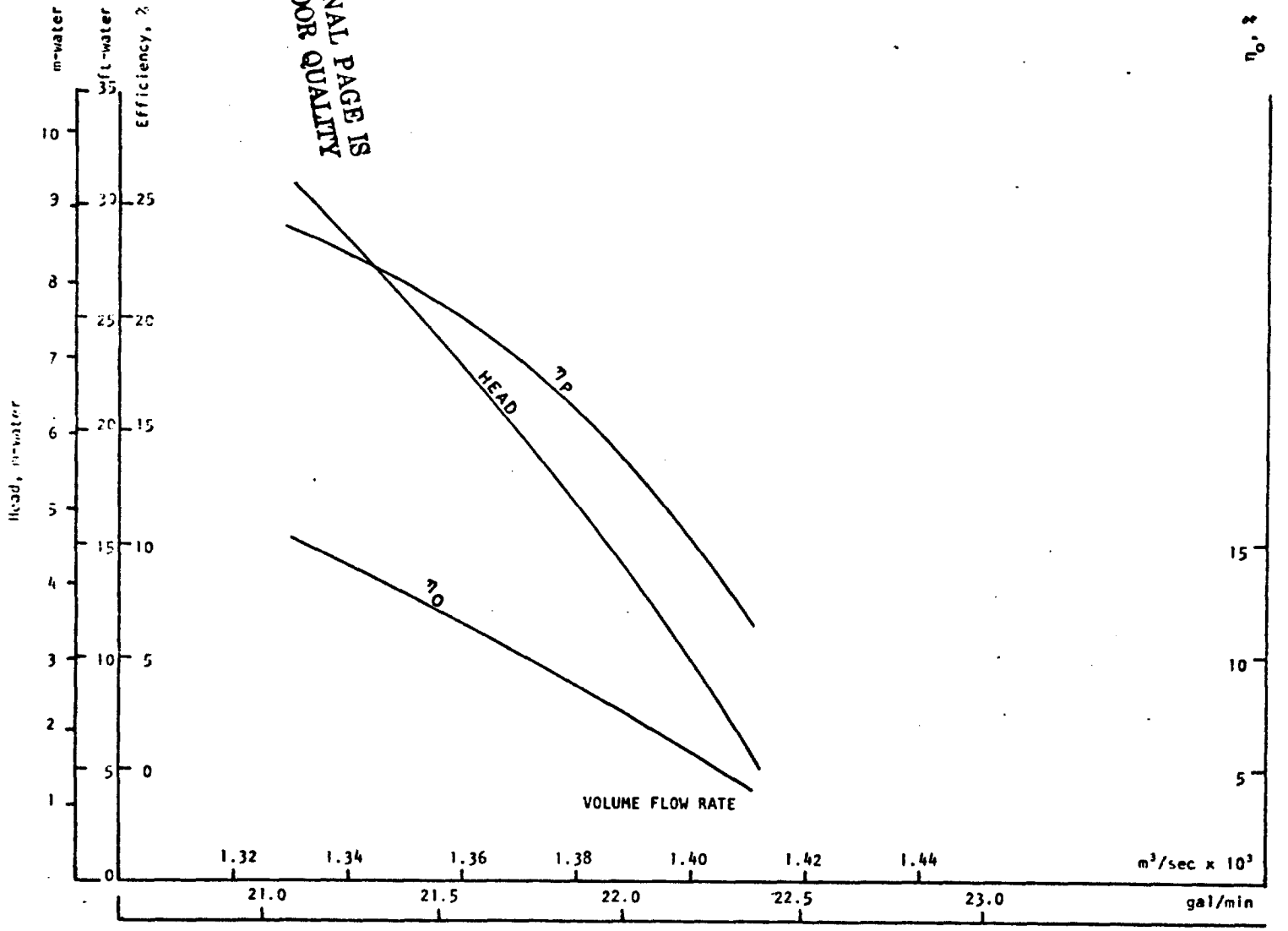

Figure 3.22. Performance Data for 1/3 hp Teel

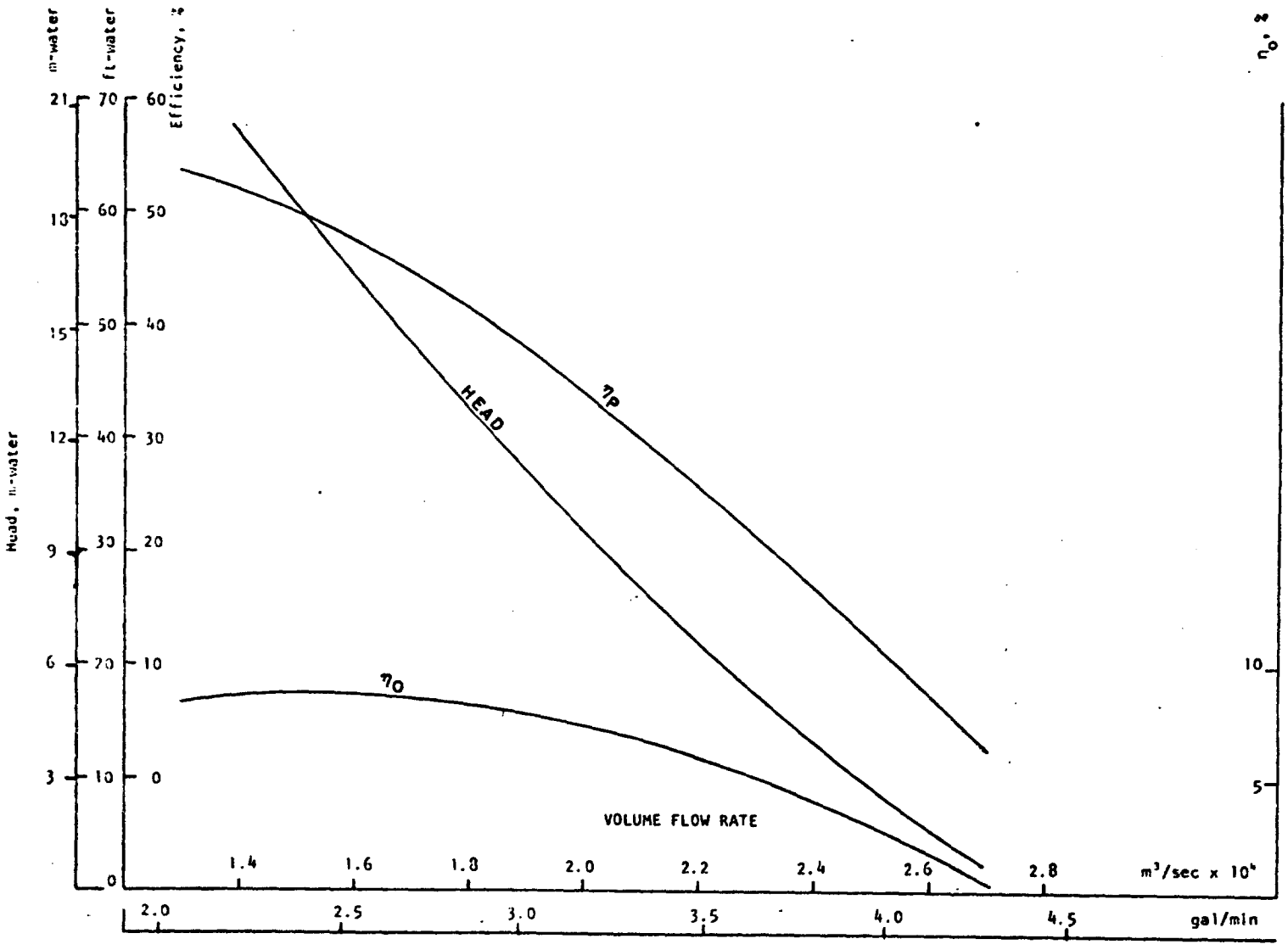

figure 3.23. Performance Data for 1/4 hp Flotec Pump

The noise level measurement of the complete line of Bell and Gossett pumps ranged from 73 dBA for the one-fourth horsepower pump to 86 dBA for the one-horsepower pump. The one-third horsepower pump had a 79 dBA noise level. This was essentially the same as the 82 dBA for the Taco and 84 for the Myers and Burk. The Grunfos 185-watt pump had a 73 dBA reading. All of the centrifugal pumps produced a noise level which is within the permissible level of 90 dBA for eight-hour exposure given in reference [12].

The noise level for the positive displacement pumps was measured at the relatively-high rotational speed of all tests (1720 rpm). The values are: Teel (1/3 hp) -106 dBA, Oberdorfer (1/2 hp) -96 dBA, Brown and Sharpe (1/3 hp) -88 dBA. These all bordered on the non-permissible level for occupied spaces in residences. The positive displacement pumps were tested at only one speed since their noise level measurements were sufficiently higher than those for the centrifugal pumps that the latter appear to be preferable for residential systems, particularly from a viewpoint of noise consideration.

ORIGINAL PAGE IS
OF POOR QUALITY

CONCLUSIONS

Generally, the results of this study reveal that significant variations in overall pumping system efficiency may occur from one manufacturer to another. They also indicate the significant error associated with assuming a high pumping efficiency for smaller-sized pumps. Centrifugal pumps smaller than 1/4 horsepower were found to be very inefficient. For those cases where it was possible to separately measure the efficiency of the electric motors on the smaller pumps, they were found to have efficiencies of less than 40% which resulted in an overall efficiency in some cases of less than 10%. Additional discussions of the conclusions are presented below.

Efficiency: A summary of the peak efficiencies for the complete line of Bell and Gossett pumps which were tested is given in Table 3.12. Also included in the table are the sound level measurements. It can be seen that the general observation that a reduction in efficiency occurs as the size is lowered is substantiated by these data. This size effect phenomena appears to be less pronounced and, indeed, slightly reversed above 1/2 hp.

Table 3.12. Summary of Peak Experimental Efficiencies for Bell and Gossett Pumps and Sound Level Measurements

Size, HP	η_p, %	η_o, %	dBA
1/4	50	23	73
1/3	56	32	79
1/2	73	41	76
3/4	70	39	82
1	--	36	86

As a matter of interest, the overall efficiency for the Bell and Gossett pumps obeyed the similarity equations which are outlined in the appendix.

As a comparison of similar-sized pumps from different manufacturers, Table 3.13 presents the results of the experimentally-determined peak efficiencies for the one-third horsepower centrifugal pumps as well as a 1/12 and a 1/4 hp pump which were tested. It is not claimed that any statistical interpretation can be made, but the data indicate comparative results for a single sampling. Also shown in Table 3.13 are the efficiencies for four positive-displacement pumps. The sound level measurements are included also. The positive displacement pumps were operated at high-rotational speeds (1720 rpm), they produce less noise at lower rotational speeds, but their efficiencies decrease as the speed is lowered as evidenced by the data in Figure 3.7.

Table 3.13. Comparison of Peak Efficiencies and Noise Levels for a Sampling of Pumps from Different Manufacturers

Manufacturer, Size (HP)	η_μ, %	η_o, %	dBA
CENTRIFUGAL			
Bell and Gossett, 1/3	56	32	79
Myers, 1/3	79	34	84
Taco, 1/3	37	17	82
Burk, 1/3	58	26	84
Grundfos, 1/12	--	20	73
POSITIVE DISPLACEMENT			
Oberdorfer, 1/3	47	17	96
Brown and Sharp, 1/3	56	16	88
Teel, 1/3	27	15	106
Flotec, 1/4	53	8	---

ORIGINAL PAGE IS OF POOR QUALITY

Flow Control: During the course of the overall effort devoted to the study of pump performance, tests were conducted on a centrifugal pump and a positive displacement pump to determine the relative effects of throttling and by-passing in order to control the flow rate delivered to a load. Data for the positive-displacement pump are included in this report in Figures 3.8 and 3.9. The centrifugal pump data have not been included here. The basis of comparison was to determine the efficiency using each of the control schemes while providing

the same flow rate as that delivered to the load. In the by-pass mode the pump handled a larger flow rate than that being delivered to the load. For all cases examined, it was more efficient to throttle the flow to the desired capacity than it was to by-pass the flow. This conclusion agreed with predictions made by Griggs [14] for a centrifugal pump.

Noise: Based on the noise level measurements shown in Tables 3.11 and 3.12, it appears that centrifugal pumps are in general less noisy than positive-displacement pumps. The noise levels determined for some of the positive-displacement pumps operating at 1720 rpm exceeded the recommended permissible exposure levels of 90 dBA which is listed in Table A.1 for reference. Again, it should be noted here that the measurements were made at a distance of one inch from the pump. Consequently, it is doubtful that noise levels of this magnitude would be experienced.

Design Suggestions: The engineering designer of pumping systems in the size range examined in this work can use the data of Tables 3.11 and 3.12 to obtain a general idea of expected performance. More specific data can be obtained from the actual pump characteristic curves shown in the figures.

The head-capacity requirements of a solar application should be carefully matched with the pumping system characteristics so that the pump operates at peak efficiency and very little throttling will be required. It is better to select a flow at a higher than necessary rate through the collector, than it is to reduce flow by throttling to match pump characteristics.

The location in the fluid loop of the pump inlets which were tested is shown in the two experimental arrangements of Figures 3.1 and 3.2. The potential cavitation problem was reduced by locating the pump so that it had a positive head, streamlining the inlet geometry and the fact that water at 66°F has a low vapor pressure. For a particular solar fluid loop design, all of

these factors should be carefully examined. Careful attention by the designer to these discussed parameters can significantly reduce energy usage and improve pumping train performance.

Study Results Summary

This study was not directed at ranking or recommending specific available pumps for use in solar systems. The primary goal was to assess trends in factors affecting energy usage in typical prime movers which might be used in liquid transport solar systems. Since this is not a comprehensive study, using only arbitrarily-selected pumps, the reader is cautioned against selecting a pump from this report based purely on the data contained herein. In particular, important aspects of pump selection such as durability, materials compatability, safety, and other significant features were not addressed in this study. Also as indicated, only a small arbitrary selection of a representative cross section of available pumps were tested, so that other pumps not tested may exist which are superior to those reported herein.

Even though the quantity of types of and varieties of manufacturers of pumps tested were limited, examination of these data do imply the following:

- Pumping flow rates and head requirements should be carefully evaluated for solar systems to assure optimum pumping efficiency and minimum power consumption.
- Designers should acquire specific overall pumping train efficiency data for each pump he is considering for application before making a selection. This should be done in lieu of using typical data because of the large variations in pump performance depending on the manufacturers of the pumps.
- The pump for a solar collector should be sized to provide a satisfactory flow. When the optimal flow lies between two available pump sizes, the larger pump should be selected and no throttling should be introduced.
- If flow control is necessary, the use of throttling as the flow control technique is superior to that of by-passing from a minimum energy usage viewpoint.

- If no flow control is necessary once the best pump size is selected, no obstructions should be placed in the line to reduce the flow rate in the event higher than design flow rates result.

- Although gear pumps are slightly noisier than centrifugal pumps, the noise level for either is expected to be acceptable for most applications.

REFERENCES

1. G. S. Settles, J. T. Hamrick, W. J. Barr and M. Summerfield, "Energy-Efficient Pump Utilization," Journal of Energy, Vol. 1, No. 1, January 1977, pp. 65-72.

2. "Fluids Engineering Division News," ASME, Vol. 13, No. 1, March 1976, p. 5.

3. Pump Manual, AIChE Pump Subcommittee, 1960.

4. Hicks, T. G., Pump Selection and Application, First Edition, McGraw-Hill Book Company, Inc., New York, 1957.

5. Shepherd, D. G., Principles of Turbomachinery, The Macmillian Company, New York, 1956.

6. Lazarkiewicz, S. and Troskolanski, A. T., Impeller Pumps, Pergamon Press, London, 1965.

7. Addison, H., Centrifugal and Other Rotodynamic Pumps, Third Edition, Chapman and Hall, London, 1966.

8. Pump Engineering Data, Economy Pumps, Inc., Hamilton, Ohio, 1945.

9. Hydraulic Institute Standards for Centrifugal, Rotary and Reciprocating Pumps, Twelfth Edition, New York, 1969.

10. Stepanoff, A. J., Centrifugal and Axial Flow Pumps, John Wiley and Sons, Inc., New York, 1957.

11. MacGregor, C. and Csomor, A., "Rotating and Positive-Displacement Pumps for Low-Thrust Rocket Engines," NASA CR-72965, R-8494-1, Final Report, Vol. 1, Evaluation and Design, 1974.

12. "Occupational Noise Congrol," W. B. Swim, Division of Occupational and Radiological Health, Department of Public Health, State of Tennessee, Nashville, Tennessee, 1975.

13. Griggs, E. I., Personal Communication, Tennessee Technological University, Cookeville, Tennessee.

14. "Noise, the Environmental Problem, a Guide to OSHA Standards," OSHA 2062, Occupational Safety and Health Administration, U.S. Department of Labor, 1972.

ORIGINAL PAGE IS
OF POOR QUALITY

APPENDIX

A brief survey of pump types, operating characteristics and theoretical background is given in this appendix. In addition discussions of efficiency, cavitation and noise are presented.

PUMP TYPES AND OPERATING CHARACTERISTICS

Four items of primary interest when studying pump performance are head and flow capacity, overall efficiency, cavitation, and noise. The head and capacity characteristics are best discussed with respect to the different types of pump design. These are presented in this section for positive displacement pumps and for kinetic pumps. The theory of operation of each type is outlined. Then, considerations of general pump efficiency are discussed, followed by brief discussions of cavitation problems and noise constraints.

Two main pump classifications are positive displacement and kinetic [3].* Two different types of positive displacement pumps include:

1. Reciprocating
2. Rotary
   a. Gear
   b. Cam and piston
   c. Screw
   d. Vane
   e. Wobble plate

The kinetic pump types are:

1. Centrifugal or radial
2. Mixed flow
3. Axial flow [2]

Positive Displacement Pumps

The positive displacement pump operates on the principle of trapping a volume of fluid in the pump and applying a mechanical force to push it through

*Number in brackets in this appendix designates the references listed at the end of the report.

the system. The losses due to fluid friction in the pump are small. Although the flow rates for these pumps are rated from zero to several hundred gallons per minute, there is no problem in finding one to operate in the range of typical solar applications. Pressure is developed according to the head requirements of the system. Low heads reduce the power requirements. The flow rate range is controlled by the rotational speed of the pump. A set of pulleys and a V-belt can be used to couple the motor-pump system for the desired operating range.

General characteristics of positive displacement pumps include high heads, low capacity, low efficiency at low speeds, relatively high mechanical friction and close clearance to avoid leakage. Close clearance contributes both to mechanical friction and to high local velocities in the fluid.

The reciprocating pump is a piston-cylinder arrangement with check valves and is similar in operation to the internal combustion engine. First the piston will move down creating a vacuum in the cylinder which opens a check valve to allow the fluid to enter the cylinder. When the piston moves up, the inlet check valve closes and the outlet check valve opens. The fluid is pushed out by the piston until it reaches its highest point in the cylinder and then reverses its direction. The piston then moves back down to start the cycle again. The pulsating flow can be somewhat reduced by using two or more piston-cylinder arrangements operating out of phase. Some surging still exists with two cylinders. Experience with the internal combustion indicates that smoother operation increases with 4, 6, 8, and 12 cylinders.

ORIGINAL PAGE IS
OF POOR QUALITY

Reciprocating pumps deliver a pulsating flow and for this reason are not ideally suited for solar applications. Rotary pumps, however, can supply a relatively steady circulation for the fluid. Both the reciprocating and the rotary types of positive displacement pumps must have a means for pressure relief or a by-pass system so that excessive pressures will not develop in the system if a flow blockage occurs.

Five of the commonly used rotary pumps are shown in Figure A.1.

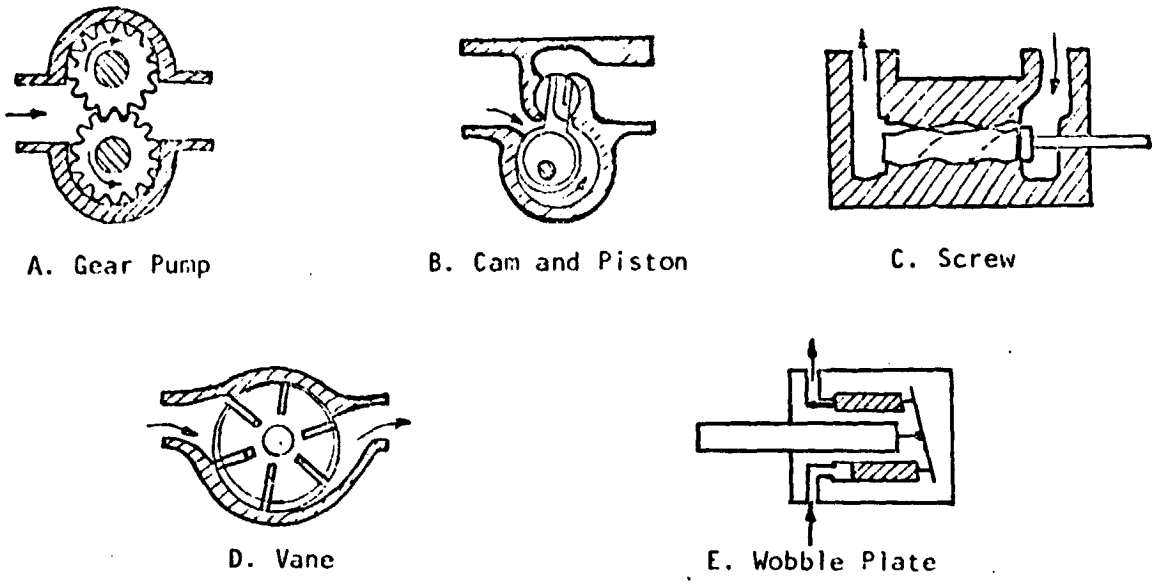

Figure A.1. Rotary Pumps

References [3, 4, 7, 9, and 11] give operational methods and performance characteristics of these positive displacement pumps. Only a short description of the operation of each is presented below to review the types of rotary pumps.

The gear pump traps the volume of fluid between the two opposing gears in the inlet section at the point when these first touch. As the gears rotate the fluid is pushed to the discharge side of the pump. The flow rate is determined by the volume trapped by each pair of gears and the rotational speed of the gears. The head generated depends on the requirements of the discharge piping. The energy required to turn the gears at a given rotational speed will increase with increase in the head required in the discharge section. At high rotational speeds the surging pressures are negligible.

The cam and piston pump is shown in Figure A.1 at the point where the eccentric cam has sealed off the inlet. When rotation continues, the spring loaded piston will move down to expose the exit port, and the trapped fluid will

be pushed through the pump. When the high point of the cam has reached the piston, the exit port is closed and a new charge of fluid is in position to be pumped. A slight pressure drop in the discharge section will be experienced at this point in the pump cycle. The surging is reduced at high rotational speeds. Flow rate and head are controlled by the same method as those for the gear pump.

The screw pump operates in a manner identical to the gear pump. The inner screw rotates at a constant speed trapping fluid between the screw and the outer fixed housing. The outer housing plays the role of the second gear in the gear pump. The construction allows for a very steady flow rate and the head is again governed by the discharge requirements and the power input into the screw.

The vane pump incorporates moveable vanes which may extend by centrifugal force or may be spring loaded. When the vanes at the inlet section are extended and touch the housing, a certain volume of fluid is trapped. Continued rotation pushes the fluid to the discharge while the housing pushes the vanes back into their slots in preparation for the next rotation. A steady discharge pressure is maintained and flow rate increases with increased rotational speed.

The wobble plate shown in Figure A.1 is attached to a piston-cylinder arrangement. The principle of operation would be the same without these elements, but the inlet and exit housing would be altered. The angle of the plate sets the volume of the piston cylinder and the flow rate for a fixed rotational speed. Increased rotational speed will also increase the flow rate. For the pump shown, the piston-cylinder component rotates while the plate and pistons wobble. The top and bottom piston will exchange relative positions for each one-half revolution. The fluid trapped in the inlet section will be forced out as the piston moves through the cylinder.

The similarity in the principle of operation for all of the above positive displacementpumps is obvious. The equations giverning their operation can be found in the references already cited and are presented here for completeness.

For a positive displacement pump the flow rate varies linearly with the rotational speed:

$$\dot{Q} = c\ N \tag{A.1}$$

where Q = volume flow rate, cubic meters/second

c = constant, cubic meters/revolution

N = rotational speed, revolutions/second

The theoretical pumping power requirement at a particular rotational speed is directly proportional to the pressure drop of the system:

$$HP = \dot{Q}\Delta P \tag{A.2}$$

where HP = power requirement, watts

ΔP = head loss for the system, Newtons/square meter

Equation (A.2) only gives the thermodynamic fluid power and does not include any inefficiencies. Since the total head generated in a positive displacement pump is independent of the flow rate, the power requirement is a function of two independent parameters. There is a functional dependence between flow rate and head loss in a specific circulation loop; however, the total pump head characteristics vary from one application to another.

The laws of similarity for positive displacement pumps are relatively simple because of the independence of the two principal parameters. The geometric size similarity between two pumps can be realized provided the pumps have the same geometry but differ in size. Another form of the equation for fluid flow rate which depends on size can be written:

$$\dot{Q} = A\ r^3\ N \tag{A.3}$$

where A = a constant (the same for geometrically similar pumps)

r = a characteristic radius of the pump

The geometric similarity laws for positive displacement pumps are

$$1) \quad \frac{Q_1}{Q_2} = \frac{r_1^3 N_1}{r_2^3 N_2} \tag{A.4}$$

$$2) \quad \frac{HP_1}{HP_2} = \frac{Q_1 (\Delta P)_1}{Q_2 (\Delta P)_2} = \frac{r_1^3 N_1 \Delta P_1}{r_2^3 N_2 \Delta P_2} \tag{A.5}$$

The efficiency relationship between a scale model and a prototype is influenced by the geometric scaling. This is discussed later in the section on efficiency.

Kinetic Pumps

The general characteristics of kinetic pumps are high capacity, low head and high rotational speed. These type of pumps generally have a stall pressure which would not damage a solar system should system blockage occur. The capacity is dependent on the head loss of the system. For many centrifugal pumps this is approximately a linear relationship [4].

The principle of operation of centrifugal pumps is to receive fluid on an impeller near the axis of rotation at the smaller diameter. This fluid is then accelerated to a high velocity by the blades and the centrifugal force moves the fluid from the axis of the impeller to the larger outer diameter. At this point it has a high velocity and a high kinetic energy. The fluid then enters a diffusing section which changes the kinetic energy into static pressure. More details of the principle of operation are presented below via application of the Euler turbine equation to a single impeller blade.

The axial flow pump is sometimes called a propeller pump because it develops the flow and head by the lifting action of the blade on the field. An axial pump does not change the direction of fluid flow between the inlet and exit. The centrifugal pump generally changes the direction of fluid flow through ninety degrees from the inlet to the impeller to the impeller exit. The axial

ORIGINAL PAGE IS
OF POOR QUALITY

flow system has a higher capacity, but it is limited to very low heads. This probably reduces its potential for application in solar systems. No commercially available pumps of this type were found in this study with the desired head-capacity characteristics. Figure A.2 shows the radial-flow centrifugal pump and the axial-flow pump.

The mixed flow systems are essentially the same as centrifugal pumps. They have some axial component of forced flow, but they perform about the same as the centrifugal systems. The lift component of the mixed flow pump is identical to that of the axial pump, but most mixed flow pumps obtain most of their head from centrifugal pumping action. The angle between the inlet and exit of the fluid being pumped is generally less than ninety degrees. Therefore, the principle of operation of the mixed flow pump involves a combination of the centrifugal and axial-flow principles, but it is usually more dependent upon centrifugal action.

Most analyses of kinetic pumps are the same for the three different types. This section is devoted to a development of the centrifugal pump equations. The Euler turbine equation can be used to represent centrifugal pumps in the form:

$$\Delta H = (U_1 V_{T_1} - U_2 V_{T_2})/g \qquad (A.6)$$

where ΔH = change in the head of the fluid, meters

g = local acceleration of gravity, meters/second squared

U_1 = linear velocity at radius, r_1, meters/second

U_2 = linear velocity at radius, r_2, meters/second

V_{T_1} = tangential velocity component of the fluid leaving the pump at radius, r_1, meters/second

V_{T_2} = tangential velocity component of the fluid entering the pump at radius, r_2, meters/second

An alternate form of Equation A.6 is

$$\Delta H = \frac{N}{g}(r_1 V_{T_1} - r_2 V_{T_2}) \qquad (A.7)$$

ORIGINAL PAGE IS
OF POOR QUALITY

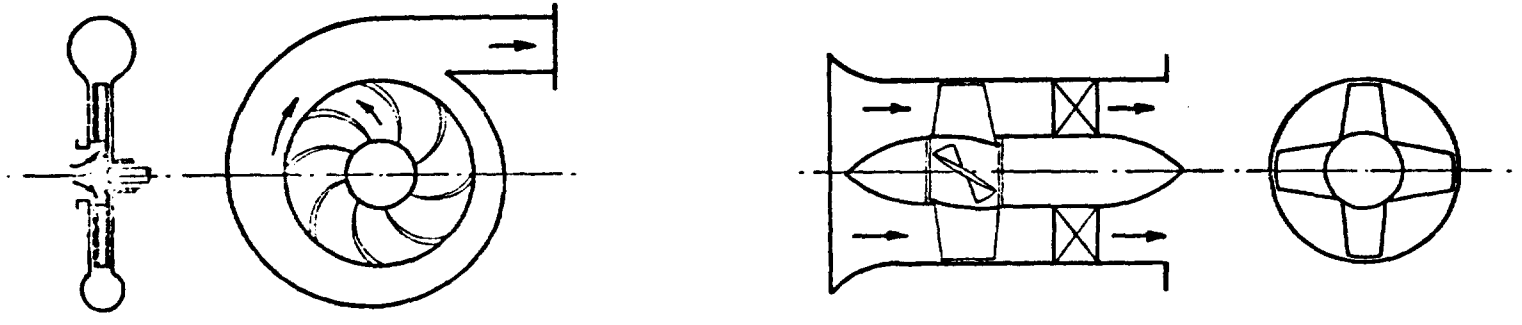

A. Centrifugal Pump

B. Axial-Flow Pump

Figure A.2. Kinetic Pumps

The tangential component of fluid velocity depends primarily on the curvature of the impeller. Impellers may be forward turned (high pressure), radial, or backward turned (lower pressures).

A simplification of the Euler equation can be made to appropriximate the effect of change in head on the volume flow rate. If the inlet velocities are negligible, Equation A.6 becomes

$$g\Delta H = U_1 V_{T_1} \tag{A.8}$$

Also the true tangential component of velocity, V_{T_1}, is the vector difference between the absolute velocity of the rotor tip and the radial component (see Figure A.3). Then,

$$V_{T_1} = U_1 - (V_{r_1})(\cos \beta) \tag{A.9}$$

where V_{r_1} = the velocity projected along the impeller blade

β = the angular curvature of the vane at the exit.

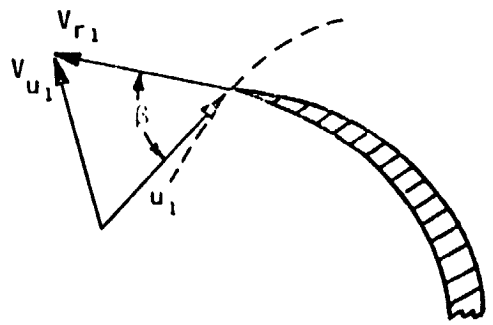

Figure A.3. Impeller Velocity Diagram

The net velocity of the fluid in the radial direction is $V_{r1} \sin\beta$. And the net volume flow rate would be

$$Q = V_{r_1} \sin \beta \, A_1 = V_{m_1} A_1 \tag{A.10}$$

where A_1 = area of the exit passage, square meters

V_{m_1} = mean exit flow velocity

Then, equation A.8 becomes

$$g\Delta H = U_1^2 - U_1 (V_{m_1} \cot \beta)$$

$$= U_1^2 - \frac{U_1 \dot{Q}_1 \cot \beta}{A_1} \tag{A.11}$$

Since $U_1 = r_1 N$, the head is related to the capacity by the linear equation:

$$g\Delta H = C_1 - C_2 \dot{Q} \tag{A.12}$$

The thermodynamic fluid power requirement is given by

$$HP = \dot{Q} \Delta H \rho g \tag{A.13}$$

where ρ = density of the fluid with head ΔH, $Kg/meter^3$

The volume flow rate, given by equation (A.10), indicates that the capacity varies linearly with the rotational speed of the pump. The flow rate-speed performance relationship is

$$\frac{\dot{Q}_1}{\dot{Q}_2} = \frac{N_1}{N_2} \tag{A.14}$$

Since C_1 of equation (A.12) varies with the square of rotational speed and C_2 varies linearly with rotational speed, the head varies as the square of the rotational speed. This is expressed by

$$\frac{\Delta H_1}{\Delta H_2} = \frac{N_1^2}{N_2^2} \tag{A.15}$$

The effective fluid power requirement then varies as the cube of the rotational speed.

$$\frac{HP_1}{HP_2} = \left(\frac{N_1}{N_2}\right)^3 \tag{A.16}$$

The last three equations (A.14-A.16) govern the variation of performance of a pump with rotational speed.

ORIGINAL PAGE IS
OF POOR QUALITY

Pump Efficiencies

Pump efficiency is defined to be the fluid power done by the pump ($\rho g \dot{Q} \Delta H$) divided by the shaft power input to the pump. Many of the smaller pumps are directly coupled to an electric motor. In testing these systems, the overall efficiency is used. This is the ratio of the fluid power of the pump to the electrical input power.

Figures A.4 and A.5 are typical of pump efficiency curves supplied by manufacturers. To obtain an overall efficiency from this data, the pump efficiency must be extrapolated (using similarity laws or by approximation) and multiplied by an assumed efficiency of the electric motor and coupler used in driving the pump.

For a particular pump the efficiency goes to zero as the capacity goes to zero. It would be necessary to use similarity laws between pumps of identical geometrical design but dimensionally scaled down to predict the efficiencies at low capacities. Theoretically the similarity calculations could be accomplished from the equations: (Reference 6)

$$\dot{Q} \propto Nd^3$$

$$\Delta H \propto N^2(d)^2$$

$$HP \propto N^3(d)^5 \qquad \text{(A.17)}$$

where d = pump vane diameter, meters

These equations apply only to centrifugal pumps. They could be used to predict the pump performance of a smaller pump based on data from a particular pump. Data from a curve such as Figure A.5 at the peak efficiency value on the curve would be used to predict the flow of a scale model pump of the same geometric design. The equation is

$$\frac{\dot{Q}}{\dot{Q}_s} = \frac{N(d)^3}{N_s(d_s)^3} \qquad \text{(A.18)}$$

where the subscript s refers to the scaled pump.

One dimensionless number which should be preserved for similarity is the kinematic specific speed which is defined by

$$\eta_s = \frac{N\dot{Q}}{(\Delta H)^{3/4}} \qquad \text{(A.19)}$$

Similarity requires that

$$\eta_{s1} = \eta_{s2}$$

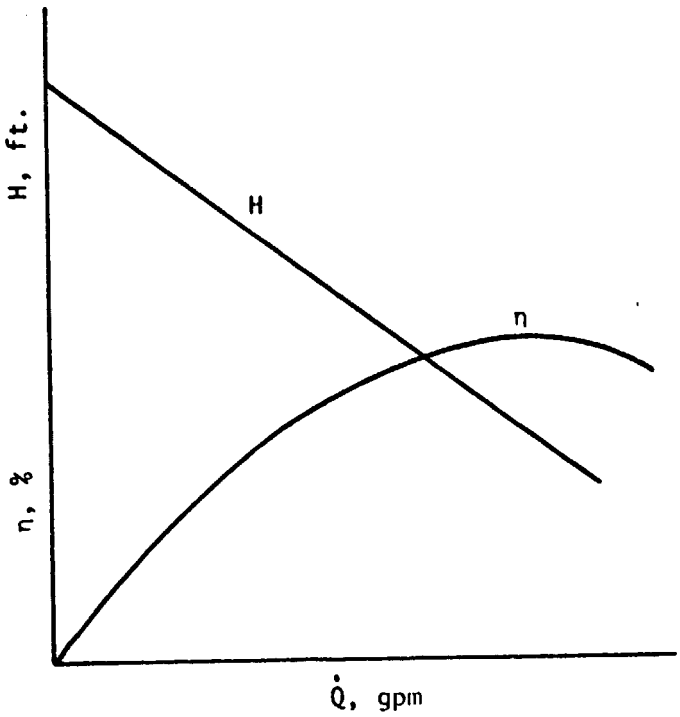

Figure A.4. Performance Curve

ORIGINAL PAGE IS
OF POOR QUALITY

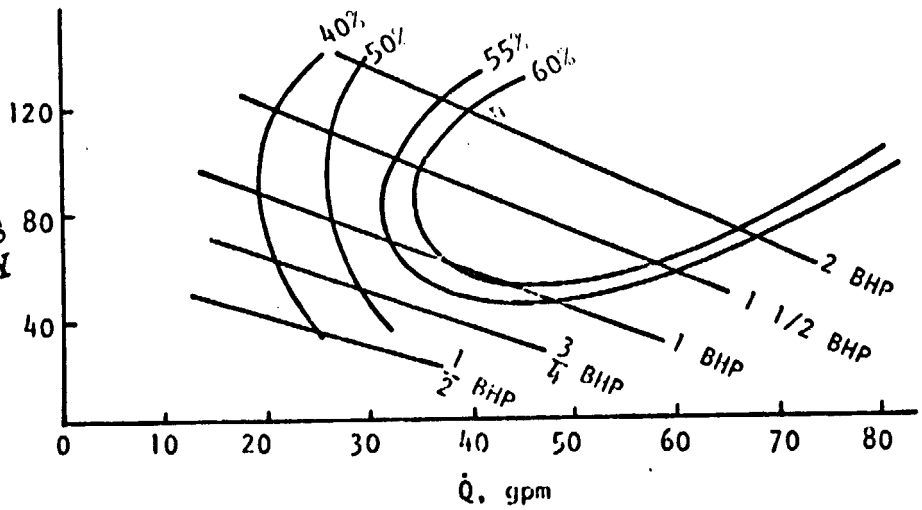

Figure A.5. Typical Efficiency Curve

If two different size pumps of the same geometry are to be compared for flow of the same liquid, the condition of similarity of flow is that the values of dynamic specific speed be the same for the two pumps. Dynamic specific speed is defined by

$$\eta_{sp} = \frac{N\ HP}{(\Delta H)^{3/4}} \tag{A.20}$$

Similarity then requires that

$$\eta_{sp_1} = \eta_{sp_2} \tag{A.21}$$

Cavitation

All pumps have the same problem with cavitation, independent of the pump design. When the static pressure in the fluid becomes less than the vapor pressure of the fluid at the fluid temperature, local vapor bubbles develop. This creates the problems of reducing mass flow rate and very high localized pressures when the vapor bubble collapses. The positive displacement pumps are generally less affected by cavitation than are the kinetic pumps.

Since solar energy systems frequently pump high temperature water, they are likely to experience cavitation. The net positive suction head of a pump is defined by the equation:

$$NPSH = h_a + h - h_v \tag{A.22}$$

where h_a = atmospheric head

h = total local head

h_v = vapor pressure head

Pumps in solar systems can be located so that the total local head is a positive number. It is the sum of the local static head, h_s, the dynamic head, $V_1^2/2g$, a fraction of the relative pump dynamic load, $c_1 V_r^2/2g$, and the friction head, h_f.

$$h = h_s + \frac{V_1^2}{2g} + c_1 \frac{V_r^2}{2g} + h_f \tag{A.23}$$

where h_f is the friction head loss between the fluid surface and pump impeller

V_r is a relative velocity between pump rotor and fluid.

It is not usually possible to determine V_r analytically. The value of h_f is dependent upon the piping geometry between fluid surface and pump inlet. Therefore, h is known to depend upon h_f, V_r, and c_1, but the specific values of this parameter may not be known.

Cavitation is assumed to start when the vapor head equals the sum of the static head and the atmospheric head:

$$h_v = h_s + h_a$$

$$= h_a + h - h_f - \frac{V_1^2}{2g} - c\ \frac{V_r^2}{2g} \qquad (A.24)$$

Then,

$$NPSH = h_f + \frac{V_1^2}{2g} + c\ \frac{V_r^2}{2g} \qquad (A.25)$$

If the local barometric pressure is one standard atmosphere, and water at 373°K is the fluid, the vapor head is equal to the atmospheric head. Then the static head must be positive.

$$h_s = h = \frac{V_1}{2g} - c_1\ \frac{V_r^2}{2g} - h_f \qquad (A.26)$$

The total head is the vertical distance between the pump inlet and the liquid level in the storage tank for the solar system. The two velocity factors are dependent on the fluid flow rate. The friction head can be reduced by placing the pump as close to the storage tank as possible. It is also desirable to avoid small diameter pipe, valves, and elbows between the tank and the pump. For the case where $h_v = h_a$ (i.e., open storage tank, water at 373°K), the static head must be positive. This would require that the flow rate be less than that of free flow from the tank.

Thermal stratification in the storage tank would cause the cooler fluid to be pumped first if the fluid were removed from the bottom of the tank.

ORIGINAL PAGE IS
OF POOR QUALITY

However, operation at high temperatures would have a high probability of cavitation unless the system was pressurized.

The ratio of NPSH to total head developed by the pump is called Thoma's cavitation parameter, σ: [5]

$$\sigma = \frac{NPSH}{\Delta H} \tag{A.27}$$

Since NPSH varies significantly with pump design, tests for each pump must be performed to determine the value of σ for which cavitation occurs.

Noise

The Federal Occupational Safety and Health Act (OSHA) became law in 1970. The laws relative to noise are included in reference [14]. A summary of permissible noise exposure levels is given in reference [12] and is shown in Table A.1.

Table A.1. Permissible Noise Exposures

Duration Per Day, Hours	Sound Level dBA Slow Response
8	90
6	92
4	95
3	97
2	100
1.5	102
1	105
0.5	110
.25 or less	115

Summary

Methods of predicting pump performance for both positive displacement and kinetic pumps are available using the equations outlined in this appendix; however, the equations generally require one set of pump characteristics such as those of Figure A.4. When a particular pump has characteristics like those shown in Figure A.4, for example, the performance of a geometrically similar pump (either larger or smaller) can be predicted. Equations A.4 and A.5 would

be used for positive displacement pumps, and equations A.18, A.19, and A.20 would be used for centrifugal pumps. The similarity equations for axial pumps and those for mixed flow pumps are not included in this appendix.

ORIGINAL PAGE IS
OF POOR QUALITY

Nomenclature

A	a constant for a particular pump
A_1	area of exit passage, square meters
c	constant, cubic meters/revolution
c_1	constant in relative dynamic load
C_1	constant for the heat equation
C_2	constant for the head equation
d	pump vane diameter, meters
EPH	electrical power measurement, watts
g	local acceleration of gravity, meters/square second
h	total head, meters of fluid
h_a	atmospheric head, meters of fluid
h_f	friction head, meters of fluid
h_s	static head, meters of fluid
h_v	vapor pressure head, meters of fluid
HP	power, watts
ΔH	change in the head of the fluid, meters of fluid
N	rotational speed, revolutions/second
NPSH	net positive suction head
ΔP	head loss for the system, Newtons/square meter
$\dot{Q}$	volume flow rate, cubic meters/second
r	a characteristic radius of a pump
U_1	linear velocity at radius, r_1, meters/second
U_2	linear velocity at radius, r_2, meters/second
V_1	fluid velocity, meters/second
V_{m_1}	mean exit velocity, meters/second
V_r	relative velocity between pump and motor, meters/second
V_{r_1}	velocity projected along the impeller blade

V_{T_1} tangential velocity component leaving pump at, r_1, meters/second

V_{T2} tangential velocity component entering pump at, r_2, meters/second

Greek letters

β angular curvature of the vane at the exit

η calculated efficiency

η_e electric motor efficiency

η_L Moody mean efficiency for large pump

η_m Moody efficiency factor

η_o overall efficiency, $\dot{Q}\Delta H/HP$

η_p pump efficiency, η/η_e

η_s kinematic specific speed, $N\sqrt{\dot{Q}}/(\Delta H)^{.75}$

η_{sp} dynamic specific speed, $N\sqrt{HP}/(\Delta H)^{1.25}$

$\Delta\eta/\eta$ measured root sum square error analysis

ρ density of the fluid flowing

σ Thoma's cavitation parameter

Subscripts

s scaled pump

☆ U. S. GOVERNMENT PRINTING OFFICE 1978—740-193/327 REGION NO. 4